Molecular role of RNF43 in canonical and noncanonical Wnt signaling

Tadasuke Tsukiyama[a], Akimasa Fukui[b], Sayuri Terai[a], Yoichiro Fujioka[c], Keisuke Shinada[a], Hidehisa Takahashi[a], Terry P. Yamaguchi[d], Yusuke Ohba[c], and Shigetsugu Hatakeyama[a]

Department of Biochemistry, Hokkaido University Graduate School of Medicine, Sapporo, Hokkaido, Japan[a]; Laboratory of Tissue and Polymer Sciences, Division of Advanced Interdisciplinary Science, Faculty of Advanced Life Science, Hokkaido University, Sapporo, Hokkaido, Japan[b]; Department of Cell Physiology, Hokkaido University Graduate School of Medicine, Sapporo, Hokkaido, Japan[c]; Cancer and Developmental Biology Laboratory, Center for Cancer Research, National Cancer Institute-Frederick, NIH, 1050 Boyles St., Bldg. 539, Rm. 218, Frederick, Maryland, USA[d]

Running title: Molecular role of RNF43 in Wnt signaling

#Address correspondence to Shigetsugu Hatakeyama, hatas@med.hokudai.ac.jp

Word count for the Materials and Methods section: 1,934

Combined word count for the Introduction, Results and Discussion sections: 4,680

ABSTRACT

Wnt signaling pathways are tightly regulated by ubiquitination, and dysregulation of these pathways promotes tumorigenesis. It has been reported that the ubiquitin ligase RNF43 plays an important role in frizzled-dependent regulation of the Wnt/βcatenin pathway. Here, we show that RNF43 suppresses both Wnt/βcatenin signaling and noncanonical Wnt signaling by distinct mechanisms. The suppression of Wnt/βcatenin signaling requires interaction between the extracellular PA domain and the CRD of frizzled and the intracellular RING-finger domain of RNF43. In contrast, these N-terminal domains of RNF43 are not required for inhibition of noncanonical Wnt signaling, but interaction between the C-terminal cytoplasmic region of RNF43 and the PDZ domain of dishevelled is essential for this suppression. We further show the mechanism by which missense mutations in the extracellular portion of RNF43 identified in patients with tumors activate Wnt/βcatenin signaling. Missense mutations of RNF43 change their localization from the endosome to the ER, resulting in the failure of frizzled-dependent suppression of Wnt/βcatenin signaling. However, these mutants retain the ability to suppress noncanonical Wnt signaling probably due to interaction with dishevelled. RNF43 is also one of the potential target genes of Wnt/βcatenin signaling. Our results reveal the molecular role of RNF43 and provide an insight into tumorigenesis.

INTRODUCTION

The mammalian *Wnt* gene family encodes nineteen cysteine-rich secreted signaling molecules that regulate essential functions during embryogenesis (1). Wnts are also required for the maintenance of adult tissues and, when misregulated, can promote tumorigenesis and other diseases (2-6). These Wnts are classified into two subclasses, Wnt1- and Wnt5a-class Wnts, based on their downstream signaling (7).

Firstly, Wnt1-class Wnts, "canonical Wnts", lead to βcatenin accumulation and 2º axis formation when their mRNA are injected into *Xenopus* embryos (8). βcatenin is the primary transducer of canonical Wnt/βcatenin signals and is the principal component of the well-characterized canonical Wnt/βcatenin signaling pathway. In the absence of a Wnt-mediated signal, the βcatenin degradation complex, which includes adenomatous polyposis coli (APC), axin, casein kinase Iα (CKIα) and glycogen synthase kinase 3β (Gsk-3β), phosphorylates cytoplasmic βcatenin, resulting in ubiquitin-proteasome-dependent degradation by $SCF^{\beta TrCP}$ ubiquitin ligase (9). Binding of some canonical Wnt family members to the Frizzled receptor and the lipoprotein receptor-related protein (LRP) 5 and LRP6 co-receptors targets βcatenin degradation complex to the cell membrane via Axin, resulting in the inhibition of Gsk-3β and the accumulation of unphosphorylated active βcatenin. Nuclear translocation of active βcatenin and binding to the T cell factor (Tcf) family of HMG box-containing transcription factors such as Tcf1 and lymphoid enhancer-binding factor 1 (Lef1) displace co-repressors of the groucho-related gene family (10), convert Tcfs from

repressors to activators, and thereby activate target genes including c-myc that maintains cells in an undifferentiated state.

Secondly, Wnt5a-class Wnts, "noncanonical Wnts", do not induce 2º axis formation but lead to axis shortening when their mRNA are injected into *Xenopus* embryos (8). Indeed, mouse embryos that lack Wnt5a expression displayed a short axis phenotype including anterior-posterior and distal-proximal axes, indicating that noncanonical Wnts regulate convergent extension (CE) movement to elongate axes (11). Noncanonical Wnts do not cause accumulation of βcatenin or induction of target genes but confers cell polarity and induces cell migration through the Wnt/Ca^{2+} pathway and/or Wnt/JNK pathway (5). In addition, it has been reported that Wnt5a antagonizes Wnt/βcatenin signaling at levels of the Wnt receptor (12), leads to degradation of βcatenin in a phosphorylation-independent manner by inducing the expression of the ubiquitin ligase Siah1/2 (13-15), and phosphorylates Tcf/Lef transcription factors to eliminate them from the nucleus via the Wnt5a-TAK1-NLK-Tcf/Lef pathway (16, 17). Therefore, Wnt5a suppresses the target genes of Wnt/βcatenin signaling and acts as a tumor suppressor.

Constitutive activation of the mammalian Wnt/βcatenin pathway is strongly associated with mouse and human cancers (18). This is particularly well-characterized in colorectal cancer (CRC), where it has been shown that inactivating mutations in negative regulators (e.g., components of βcatenin destruction complex) of Wnt/βcatenin signaling, such as *APC* and *Axin*, or overactivating mutations in positive regulators such as βcatenin lead to c-myc expression and tumorigenesis. Mice carrying the Apc^{Min}

mutation develop hundreds of intestinal adenomas due to the decline of βcatenin degradation and have been instrumental in understanding the role of Wnt signaling in gastrointestinal cancers.

It is well known that ubiquitin-dependent proteolysis plays an essential role in the regulation of Wnt signaling (19). Indeed, the stability of many critical components of both canonical Wnt/βcatenin and noncanonical Wnt signal transduction pathways, including Wnt receptors (20), Dishevelled (Dvl) (21-23), Axin (24, 25), adenomatous polyposis coli (APC) (26) and βcatenin (9, 13, 14), are tightly modulated by ubiquitination.

Recently, it has been reported that two of the transmembrane ubiquitin ligases, ring finger protein 43 (RNF43) and its homolog zinc and ring finger 3 (ZNRF3), ubiquitinate frizzleds (Fzds) to downregulate the surface expression of the Wnt receptor including Fzd1/2/3/4/5/8 and LRP5/6 and the activity of Wnt signaling in the absence of R-spondin, suggesting that these ubiquitin ligases act as tumor suppressors (27, 28).

Here, we show that RNF43 strongly suppressed both canonical Wnt/βcatenin signaling and noncanonical Wnt signaling through distinct mechanisms and that missense mutations in the extracellular domain of RNF43 identified in patients with tumors invert the function of RNF43 from a negative regulator to a positive regulator of Wnt/βcatenin signaling.

MATERIALS AND METHODS

Prediction of RNF43 protein structure. The amino acid sequence of RNF43 (NP_060233.3) was analyzed for the conserved domain and positions of the transmembrane and signal peptide using databases (NCBI/CCD, ExPASy/PROSITE and CBS prediction servers/TMHMM or /SignalP respectively).

Plasmids. HA epitope-tagged full-length human RNF43 complementary DNA (BC109028) in the mammalian expression vector pcDNA3-HA (pcDNA3-RNF43-HA) was described in our previous report (29). A series of deletion mutants (pcDNA3-RNF43(C, ΔR, ΔPA, ΔCPD, m1-m20, ΔR;m1, ΔPA;m1) and missense mutants (pcDNA3-RNF43(A35S, I48T, L82S, M83T, P118T, C119R, R127P, A146G, N167I, A169T, T204R and S216L)) of RNF43-HA was generated by polymerase chain reaction (PCR). PCR products amplified with KOD+ polymerase (Toyobo), pcDNA3-RNF43-HA and primers (All the primers and templates used in this study to generate expression vectors for RNF43, Fzd5 and Rspo1 are listed in Table S1) were digested by *Xho*I (m1-m3) and then self-ligated (others). RNF43 and mutants (WT, I48T, L82S and R127P) were inserted into the pEGFP-N3 vector to observe the subcellular localization of RNF43 proteins. Two synonymous substitutions (A1344G, C1353T) were introduced into pMX-puro-RNF43(WT, I48T, R127P)-HA by PCR in order to generate siRNA-resistant mutants (si;WT, si;I48T, si;R127P) for knockdown experiments. Fzd5 was tagged with an N-terminal dual FLAG epitope immediately after the signal peptide (pCS2+-FLAG-Fzd5) using PCR with KOD+ polymerase,

pCS2+-Fzd5 and primers. Two deletion mutants of FLAG-Fzd5 (pCS2+-FLAG-Fzd5(ΔCRD, CRD)) were generated using PCR with KOD+ polymerase, pCS2+-FLAG-Fzd5 and primers and then self-ligated (ΔCRD) or subcloned into pcDNA3 (CRD). pCS2-Dvl2(WT, ΔPDZ) and pEGFP-Dvl2-EGFP expression vectors were kindly provided by Dr. M. Nakaya (Yokohama City Univ., Japan) and Dr. Akira Kikuchi (Osaka Univ., Japan). Human R-spondin1 cDNA was amplified by PCR with a human prostate cDNA library and primers and then subcloned into the pFLAG-CMV5a vector (pFLAG-CMV-hRspo1).

All of the expression plasmids generated were sequenced. The expression vectors for Myc-Axin and ΔN-βcatenin were described in our previous report (9). HA-tagged wild-type and several deletion/missense mutants of RNF43 (ΔR, ΔPA, ΔR;m1, ΔPA;m1, I48T, L82S and R127P) were inserted into the pCS2+ vector for use in *Xenopus* experiments or into pMX-puro vectors to establish cells stably expressing RNF43.

Cell culture, transfection, siRNA and reagents. HEK293, HEK293T, STF293, HeLa, MCF7, HepG2, HCT116 and SW480 cells and mouse embryonic fibroblasts (MEFs) were grown in DMEM supplemented with 10% fetal bovine serum (Invitrogen). ES cells (W9.5) were kindly provided by Dr. Colin Stewart (IMB, Singapore) and grown in DMEM supplemented with 15% fetal bovine serum (HyClone, Thermo Scientific) and 1000 U/ml of leukaemia inhibitory factor (Millipore). STF293 cells were established by using the SuperTopFlash-luciferase reporter system, which was kindly provided by Dr. R. Moon (Univ. of Washington, USA). Wnt3a/L, Wnt5a/L and control Neo/L cells were kindly provided by Dr. S. Takada (NIBB, Japan) and grown in

DMEM/F-12 HAM supplemented with 10% fetal bovine serum. Wnt3a and Wnt5a-conditioned and control media were obtained from 24-h culture of these cells.

NIH3T3 and its derivative cell lines were grown in DMEM supplemented with 10% bovine serum (Gibco, Invitrogen). Transfection of plasmids was done using FuGENE HD Transfection Reagent according to manufacturer's protocol. Retroviral expression vectors containing HA-tagged RNF43 cDNAs (WT, ΔRING, I48T and R127P) were constructed with pMX-puro. For retrovirus-mediated gene expression, NIH3T3, HEK293 or STF293 cells were infected with retroviruses produced by Plat-E or Plat-A packing cells (30). The cells were then cultured in the presence of puromycin (3 μg/ml) for 1 week. Expression of RNF43 was confirmed by immunoblot analysis.

STF293 cells stably expressing RNF43 mutants were grown in DMEM supplemented with 10% bovine serum (Gibco, Invitrogen) for knockdown-add-back experiments. siRNA to knockdown endogenous RNF43 was purchased from Dharmacon (control siRNA, D-001810-10; hRNF43 siRNA, J-007004-11) (31). Transfection of siRNA was performed using Dharmafect1 reagent according to the manufacturer's protocol. The efficiency of siRNA for endogenous RNF43 and that for exogenous siRNA-resistant RNF43 mutants were examined by quantitative RTPCR with primers for the 3' UTR of hRNF43 mRNA and by immunoblotting with indicated antibodies.

Recombinant human R-Spondin1 protein and tumour necrosis factor α (TNFα) were obtained from R&D Systems. The effective concentration of recombinant proteins has been confirmed by luciferase reporter assays.

Luciferase assay. HEK293 and HeLa cells were seeded in 24-well plates (7.5×10^4 cells) and transfected with reporter plasmids for several signaling pathways (TopFlash reporter, NF-κB reporter (cNAT-EGFP:Luc2) (32) and Notch reporter (cNotch-EGFP:Luc2; unpublished)) plasmids (100 ng/well) and Renilla reporter plasmid (2 ng/well). TRIMs, RNFs, Wnt3a (pCIG-Wnt3a) and RNF43 (pCI-RNF43, pcDNA3-RNF43-HA) expression vectors at the indicated combinations were transfected by FuGENE HD Transfection Reagent (Promega). STF293 cells were seeded in 24-well plates (5×10^4 cells) and transfected with RNF43 expression plasmids by FuGENE HD Transfection Reagent. Twenty-four h after transfection, Wnt3a CM (1/2 volume), R-Spondin1 (5 ng/ml) or TNFα (20 ng/ml) was added to the culture medium and then cells were cultured for 24 h (Wnt3a CM, R-Spondin1 or TNFα stimulation) or cultured for 48 h (transfection of pCIG-Wnt1, pCIG-Wnt3a and pCR-FLAG-NICD). The cells were harvested and lysed in 100 μl of cell culture lysis reagent, and then luciferase activities were measured using 10 μl of lysates and 50 μl of luciferase assay substrates with the Dual-Luciferase Reporter Assay System or Luciferase Assay System (Promega). The luminescence was quantified with a luminometer (GLOMAX 20/20 LUMINOMATER, Promega). The relative level of luciferase activities in empty vector-transfected cells without stimuli or with Wnt3a stimulation is defined as 1. All experiments were independently repeated more than three times to confirm the reproducibility.

RNA isolation and quantitative RTPCR. Cells and tissues were homogenized in Isogen reagent (Nippon Gene) according to the manufacturer's protocol. Reverse

transcription polymerase chain reactions (RT-PCRs) were performed in a total volume of 20 μl containing total RNA (500 ng) at 50°C for 30 min using ReverTra-Plus (Toyobo). PCR was carried out as follows: 25-28 cycles of denaturalization at 94°C for 20 sec, annealing at 60°C for 20 sec and extension at 72°C for 30 sec. The primer sequences were obtained from the PrimerBank database as follows: mouse cyclophilinA (mPpia)-forward, 5'-GAGCTGTTTGCAGACAAAGTTC-3'; mPpia-reverse, 5'-CCCTGGCACATGAATCCTGG-3'; mRNF43-forward, 5'-CCGGGTCATTTCGTGCCTC-3'; mRNF43-reverse, 5'-CCTGGTTCCTGGTAAGATGGAG-3'; mZNRF3-forward, 5'-GGCGACTATACCACCCACAC-3'; mZNRF3-reverse, 5'-CTTCACCACTCCTACCCAGC-3'; hGAPDH-forward, 5'-TCGACAGTCAGCCGCATCTTCTTT-3'; hGADPH-reverse, 5'-GCCCAATACGACCAAATCCGTTGA-3'; hRNF43-forward, 5'-CATCAGCATCGTCAAGCTGGA-3'; hRNF43-reverse, 5'-TTACCCCAGATCAACACCACT-3'; hRNF43(3' UTR)-forward, 5'-CAAGAGTGTGCTCCAGATGTGT-3'; hRNF43(3' UTR)-reverse, 5'-CTTCTAGGAAGTACGGCAAAAAGA-3'; hZNRF3-forward, 5'-GGACCCGAAACCATGCCTC-3' and hZNRF3-reverse, 5'-TCTGCACCCTTCACATACACC-3'. Quantitative PCR reactions and analyses were performed with Power SYBR Green PCR Master Mix (Applied Biosystems) using a StepOne Real-Time PCR System by the $\Delta\Delta C_T$ method with the internal control gene h*GAPDH* or m*Ppia* (Applied Biosystems).

Immunoprecipitation and immunoblot analysis. Cells or tissues were lysed with a lysis buffer containing 50 mM Tris-HCl (pH 7.6), 150 mM NaCl, 0.5% Triton X-100, aprotinin (10 μg/ml), leupeptin (10 μg/ml), 10 mM iodoacetamide, 1 mM PMSF, 0.4 mM Na_3VO_4, 0.4 mM EDTA, 10 mM NaF and 10 mM sodium pyrophosphate. The lysates were incubated on ice for 20 min and then centrifuged at 16,000 *g* for 20 min at 4°C. After determination of protein concentrations with the Bradford assay (Bio-Rad), cell lysates (20 μg/lane) were subjected to SDS-PAGE on 8-10% gel, and separated proteins were transferred to an Immobilon-P membrane (Millipore). The membranes were probed with antibodies for βcatenin (610153, BD-Transduction Laboratories), Dvl2 (3224, CST), Axin (52-1207, Zymed), HA (HA.11, Covance), Myc (9E10, Covance), FLAG (M2 and M5, Sigma), and GAPDH (6C5, Applied Biosystems). Immune complexes were detected with HRP-conjugated Abs to mouse/rabbit IgG (Promega) or Mouse TrueBlot Ultra (eBioscience) and ECL (GE Healthcare Bioscience) or Immobilon Western reagents (Millipore). The cell lysates subjected to co-immunoprecipitation experiments were incubated with the indicated antibodies for 8 h and then with protein A-Sepharose beads (GE Healthcare Bioscience) for 1 h. Beads were washed 5 times with lysis buffer and the proteins interacting with beads were eluted by boiling with SDS sample buffer for immunoblot analysis. Intensities of the signals examined were quantified using ImageJ software (NIH) and normalized by the internal loading control (GAPDH).

Protein stability assay. Cells were cultured with cycloheximide (Sigma) at the concentration of 50 μg/ml and then incubated for various times indicated in figures. Cell

lysates were then subjected to SDS–PAGE and immunoblot analysis with antibodies for FLAG, HA, c-Myc, Dvl2, NEDL1 and GAPDH.

Flow cytometry. Cells were harvested using enzyme-free cell dissociation buffer (Invitrogen) and resuspended in FACS staining buffer (PBS containing 0.05% BSA and 0.05% sodium azide). Single cell suspensions of HEK293 (1×10^5 cells) cells were stained for 45 min at 4°C with phycoerythrin (PE)-conjugated anti-Frizzled4 (145901, R&D Systems) or a combination of anti-Lgr5 (ABIN864042, antibodies-online.com) and anti-mouse IgG-Alexa488 (Molecular Probes) Abs. All analyses were performed with a FACSCalibur flow cytometer and CellQuest (Becton Dickinson) or FlowJo (TreeStar Inc.) software. All graphs are indicated with normalized scales for each histogram,

Fractionation of cellular proteins. Cells were suspended in a separation buffer (10 mM Hepes (pH 7.9), 10 mM KCl, 1.5 mM $MgCl_2$, 0.5 mM DTT, 0.25 M sucrose, phosphatase inhibitors and protease inhibitors) and lysed with a Dounce homogenizer by 40 strokes. The cell lysates were separated into nuclear (500 × g, 5 min), membrane (12,000 × g, 20 min) and cytosolic fractions (supernatant). Subcellular localizations of RNF43 were confirmed by immunoblotting using the antibodies indicated.

Microscope image acquisition. Localization of RNF43 missense mutants were examined with the expression vectors for RNF43(WT, I48T, L82S and R127P)-EGFP in HeLa cells. Cells were fixed with 2% formalin and then images of cells were taken and analyzed with BX51 fluorescent microscope, DP71 camera, DP Controller and DP Manager software (Olympus). The RNF43 expression in the intracellular compartments

was analyzed with expression vectors for RNF43(WT and R127P)-EGFP and the organelle markers (ER-DsRed2, TdTomato-Rab5, TdTomato-Rab7 and TdTomato-Rab11) in HeLa cells. Cells were fixed with 2% formalin and then images of cells were taken and analyzed with IX83-ZDC fluorescent microscope (Olympus), Rolera EM-C^2 camera (Q-imaging) and MetaMorph software (Molecular Devices). Linescan analyses were performed to confirm the localization of RNF43 in the organelles. Co-localization of RNF43 mutants and Fzd or Dvl were examined with the combination of EGFP- or HA-tagged RNF43(WT and mutants), DsRed- or FLAG-tagged Fzd5, HA-tagged RNF43(WT and mutants) and Dvl2-EGFP in HeLa cells as indicated in each figure. Cells expressing the tagged proteins were fixed with 2% formalin and then stained with anti-DYKDDDK (FLAG)-Alexa555 (3768S, CST) or anti-HA-Alexa488 (A488-101L, COVANCE) Abs. Images of stained cells were analyzed with BX51 fluorescent microscope, DP71 camera, DP Controller and DP Manager software (Olympus).

***Xenopus* experiments.** *In vitro* transcription was performed to synthesize capped mRNA with linearized pCS2+-RNF43, -RNF43(ΔR, ΔPA, ΔPA;m1 and ΔR;m1), -LacZ, -GFP or pSP64T-xWnt8a as template plasmids using an mMESSAGE mMACHINE kit (Ambion) and RNeasy mini kit (Qiagen) according to manufacturer's protocol. Several combinations of GFP, xWnt8a mRNA (10 or 0.2 pg/embryo) and/or RNF43(WT and missense mutants) mRNA (1 ng) indicated in each figure were injected into two of the ventral blastomeres of *Xenopus* embryos at the 4-cell stage to evaluate the effect of RNF43 on 2° axis formation induced by an excess of Wnt/βcatenin signaling.

Quantification of 2° axis induction was photographed at stage 37-38 and scored according to a previous report(22). An animal cap assay was performed to confirm the function of RNF43 in noncanonical Wnt signaling. mRNA (1 ng) of RNF43 or its derivative was injected into four blastomeres (animal pole) at the 4-cell stage. Animal caps were dissected at stage 8 and cultured in 1 × Steinberg's solution containing 0.1% BSA (Sigma) and 5 ng/ml recombinant human activin A. The explants were photographed at stages 18–20. Images of mRNA-injected embryos were taken with the SZX16 and DP71 system (Olympus).

Statistical analysis. Student's *t*-tests and analysis of variance (ANOVA) were used for statistical analysis of differences among samples.

URLs. Catalog Of Somatic Mutation In Cancer (COSMIC) database, http://cancer.sanger.ac.uk/cancergenome/projects/cosmic/; PrimerBank database, http://pga.mgh.harvard.edu/primerbank/; NCBI/Conserved Domain Database, http://www.ncbi.nlm.nih.gov/Structure/cdd/cdd.shtml; ExPASy/PROSITE, http://prosite.expasy.org/; TMHMM Server v. 2.0, http://www.cbs.dtu.dk/services/TMHMM/; SignalP 4.1 Server and http://www.cbs.dtu.dk/services/SignalP/.

RESULTS

Identification of a novel Wnt-regulator. To identify novel ubiquitination-dependent regulators of Wnt signaling, we screened several ubiquitin ligase family members using SuperTopFlash (STF) 293 reporter cells containing a βcatenin/Tcf reporter system. Results obtained from the reporter assay indicated that a transmembrane member of the ring finger protein (RNF) family, RNF43, strongly suppressed Wnt3a-dependent activation of the reporter, whereas other RNFs and tripartite motif (TRIM) family members did not (Fig. 1A and B). While RNF43 inhibited Wnt1-induced activation of Wnt/βcatenin signaling, it had no effect on Notch signaling and nuclear factor (NF)-κB activation, indicating that RNF43 specifically suppressed Wnt-dependent activation of Wnt/βcatenin signaling (Fig. 1C-F). To test whether RNF43 can inhibit Wnt signaling *in vivo*, we examined the activity of RNF43 in a Wnt-dependent axis duplication assay using *Xenopus* embryos. Secondary axis formation promoted by ventral *xWnt8a* mRNA injections was significantly suppressed when *RNF43* mRNA was co-injected (Fig. 1G, and Table 1). These results showed that RNF43 is a strong negative regulator of Wnt/βcatenin signaling *in vivo*.

Extracellular interaction between RNF43 and Fzd. Previous studies showed that missense mutations in the extracellular domain of RNF43 are frequently identified in patients with tumors (33, 34), suggesting an important role of this portion in the regulation of Wnt signaling and in tumorigenesis (Fig. 2A). Indeed, RNF43(ΔPA) mutant lacking the extracellular domain lost the suppressive activity for Wnt/βcatenin

signaling in a manner dependent on the surface expression of Fzd4 (Fig. 2B and C). It has been suggested that a ZNRF3 mutant lacking the RING-finger domain, ZNRF3(ΔR), upregulates the surface expression of Fzd due to its dominant negative activity (27). We also confirmed that RNF43(ΔR) accumulates endogenous Fzd4 expression at the cell surface (Fig. 1H). These results suggest that dominant negative RNF43 mutants inhibit the function of endogenous RNF43 and ZNRF3 in downregulation of Fzd and thereby lead to accumulation of Fzd at the cell surface and activation of Wnt/βcatenin signaling. Conversely, the absence of the extracellular domain of RNF43 did not increase surface Fzd4 expression and did not activate Wnt/βcatenin signaling, suggesting that RNF43(ΔPA) mutant does not have a dominant negative effect. To prove this interpretation, we examined how RNF43 recognizes Fzd. The results of co-immunoprecipitation showed that interaction between RNF43 and Fzd5 requires the extracellular portions of both proteins: the CRD of Fzd and the PA domain of RNF43 (Fig. 2D and E). In addition, direct interaction between soluble forms of CRD and PA domain, which are secreted into culture media, was detected not only in the cells but also in the culture supernatant (Fig. 2F). These results suggest that RNF43(ΔPA) mutant does not show dominant negative activity in regulation of Fzd, because of its inability to interact with Fzd, and provide an answer to the question of how RNF43/ZNRF3 regulates numerous Fzd proteins in previous studies (27, 28) and of why R-spondin can release Fzd from RNF43-dependent degradation of it.

We also confirmed the importance of the extracellular interaction *in vivo* by the injection of *RNF43(ΔPA)* mRNAs into *Xenopus* embryos. *RNF43(ΔPA)*

mRNA-injected embryos recovered normal development, whereas the embryos with injection of RNF43 mRNA lacked normal cephalogenesis, indicating that RNF43(ΔPA) is not able to suppress Wnt/βcatenin signaling (Fig. 2G). A recent report showing interaction between the extracellular domain of RNF43, Lgr5 and the CRD of R-spondin 1 (Rspo1) by structural basis analysis strongly supports our results (35).

Missense mutations of RNF43 facilitate Wnt/βcatenin signaling due to their mislocalization. We assessed the function of RNF43 carrying mutations identified in patients with tumors in the regulation of Wnt/βcatenin signaling in the presence (Fig. 3B and C) or absence (Fig. 3C) of endogenous RNF43 with siRNA. Unlike the results of a previous study (27), RNF43 knockdown upregulated Wnt/βcatenin signaling, suggesting the expression of functional RNF43 in STF293, a derivative of the HEK293 cell line (Fig. 3C). Importantly, missense mutations of RNF43 in the extracellular domain (I48T, L82S and R127P) facilitated Wnt3a-induced activation of Wnt/βcatenin signaling compared to control cells regardless of endogenous RNF43 expression in a manner dependent on the surface expression of Fzd4 (Fig. 3A-D). Expression of RNF43 missense mutants significantly accelerated the axis duplication when they were co-expressed with a small amount of xWnt8a, suggesting that these mutations change the function of RNF43 from a negative regulator to a positive regulator of Wnt/βcatenin signaling (Fig. 3E and Table 1). Furthermore, facilitation of Wnt/βcatenin signaling with several mutants (ΔR, I48T, L82S and R127P) was not due to cross-talking of noncanonical Wnt signaling to βcatenin-dependent signaling by the extraordinary context of Wnt receptors as reported previously (Fig. 3F) (12, 36-38).

To examine whether these missense mutations lead to dominant negative effects, interaction between Fzd5 and RNF43 mutants was confirmed by co-immunoprecipitation. All of the RNF43 mutants retained the ability to interact with Fzd5, indicating that missense mutations in the extracellular domain of RNF43 possibly confer a dominant negative effect in the regulation of Wnt/βcatenin signaling (Fig. 4A).

To elucidate the mechanism underlying the dominant negative effect of mutant RNF43 on Wnt/βcatenin signaling, we investigated the subcellular localizations of these mutant proteins. Missense mutations did not change the distribution of RNF43 in the membrane and nuclear fractions (Fig. 4B). In contrast, fluorescence microscopic experiments showed that dominant negative mutants of RNF43 (I48T, L82S and R127P) exhibited reticular expression, whereas wild-type RNF43 showed granular expression (Fig. 4C). Therefore, we examined the localization of Fzd5 with RNF43 expression to determine the effect of aberrant expression of mutant RNF43. None of the mutants of RNF43 examined were significantly co-localized with Fzd5, although RNF43(WT) was co-localized with Fzd, suggesting that mislocalizations of RNF43 induced by missense mutations deprive RNF43 of the ability to regulate the localization of Fzd (Fig. 4D and E). Next, we examined where RNF43 is expressed in the intracellular compartments to understand the effect of RNF43 mutants in the regulation of Wnt/βcatenin signaling. A large fraction of RNF43 was co-localized with the early endosome marker Rab5, while co-localization with the late and recycling endosome markers Rab7 and 11 was not frequently observed (Fig. 4F). The dominant expression of RNF43 in one of the “membrane fraction” early endosomes supports the results of a

previous study showing lysosomal degradation of RNF43 and Fzd through endocytosis in a steady state of the cells (28). In addition, both RNF43(I48T and R127P) mutants were dominantly co-localized with an ER marker but not with Rab5, suggesting that the RNF43 mutants are not able to spatially interact with Fzd due to their mislocalization and lose their ability to regulate Fzd and Wnt/βcatenin signaling (Fig. 4G). Besides, RNF43 mutants exhibited higher expression levels than that of RNF43 (Fig. 4A-C and 8E-G). Therefore, we next examined whether higher expression levels of these mutants originated from the stabilization of RNF43 by a protein stability assay with cycloheximide (CHX). Missense mutant proteins (I48T and R127P) were more stable than wild-type of RNF43, whereas the stability of RNF43(ΔR) mutant was similar to that of RNF43(WT) (Fig. 5A), suggesting that missense mutants of RNF43 deviate from their normal trafficking and endosome-lysosomal degradation. Next, we treated cells with a proteasome inhibitor, MG132, to examine whether RNF43 mutants are degraded by a non-lysosomal pathway. MG132 treatment increased the protein levels and ubiquitination levels of RNF43(I48T and R127P) but not those of RNF43(WT and ΔR) (Fig. 5B). These findings suggest that missense mutants are degraded via the ubiquitin-proteasome pathway (possibly by ERAD) and suggest ER localization of RNF43 mutants due to their extraordinary trafficking. Also, we stimulated cells with Wnt3a and Rspo1 to confirm the false localization of these mutants that retained the ability to interact with Rspo1 (Fig. 5C). Indeed, RNF43 mutants exhibited unresponsiveness to Rspo1, whereas Rspo1 accelerated Wnt/βcatenin signaling in wild-type RNF43-expressing cells as well as in control cells (Fig. 5D). Furthermore,

accumulation of Lgr5, which may be regulated by a trafficking mechanism similar to that for Fzd, was observed on the surfaces of mutant-expressing cells (Fig. 5E). These findings indicate that RNF43 mutants are not expressed at and do not act at the cell surface.

These findings suggest that the missense mutants we examined lack the ability to downregulate expression of Fzd due to their mislocalization, stabilization and/or dominant negative effect, resulting in failure to maintain appropriate Fzd expression at the cell surface. Our findings partially correspond to results of recent studies showing that the RNF43-Rspo-Lgr complex plays an essential role in modulation of Wnt/βcatenin signaling (39), that RNF43 mutants are not expressed at the cell surface and lack the ability to downregulate Fzd (31) and that the missense mutations we examined except L82S were not mapped in the R-spondin-binding groove (35).

RNF43 inhibits noncanonical Wnt signaling in a manner dependent on binding to Dvl. It has been shown that a homolog of RNF43, ZNRF3, inhibits not only Wnt/βcatenin signaling but also convergent extension (CE) movement, which is regulated by noncanonical Wnt signaling (27). We also observed the short axis phenotype in RNF43- or RNF43(ΔR)-injected *Xenopus* embryos in both the presence and absence of xWnt8 (Fig. 1G and Table 1). Hence, we confirmed the role of the RING-finger domain of RNF43 in *Xenopus* embryos using an animal cap elongation assay. Surprisingly, activin-induced elongation of animal cap explants was suppressed in RNF43(ΔR)-injected embryos as well as in RNF43-injected embryos (Fig. 6A). It is known that both excess and insufficiency of noncanonical Wnt signaling can lead to

failure of CE movement, and our results showed that both RNF43 and RNF43(ΔR) suppressed CE movement. These findings suggested two hypotheses. One is that RNF43(ΔR) acts as a dominant negative mutant in Wnt/βcatenin signaling and leads to an excess of noncanonical Wnt signaling, resulting in the disruption of CE movement, because previous reports have shown that both expression of Rspo3 and loss of Lgr5 cause activation of the Wnt5a-dependent Wnt/PCP pathway via Fzd (40). The other hypothesis is that both RNF43 and RNF43(ΔR) act as negative regulators in noncanonical Wnt signaling and that ubiquitinating activity originating from its RING-finger domain is not essential for the regulation of noncanonical Wnt signaling. To determine whether RNF43(ΔR) functions as a negative or positive regulator in noncanonical Wnt signaling, we examined the activation of downstream transducers with Wnt5a stimulation. At first, we evaluated the function of RNF43 in the regulation of noncanonical Wnt signaling by detecting Wnt5a-dependent phosphorylation of Dvl2, and confirmed the suppression of noncanonical Wnt signaling with wild-type RNF43. It is noteworthy that phosphorylation of Dvl2 induced by Wnt5a was not accelerated but inhibited in RNF43(ΔR) stably-expressing NIH3T3 or in HEK293 cells (Fig. 6B) despite the upregulation of Fzd at the cell surface (Fig. 1H), supporting the second hypothesis that ubiquitinating activity of RNF43 is not essential for the regulation of noncanonical Wnt signaling.

To elucidate the mechanism underlying the suppression of noncanonical Wnt signaling by RNF43, we next investigated the role of the interactions between RNF43 and Fzd via the extracellular domain by using RNF43(ΔPA) mutant. Injection of

RNF43(ΔPA) mRNA still inhibited activin-induced animal cap elongation, which was also inhibited in *wild-type RNF43* mRNA-injected embryos (Fig. 6C), despite that RNF43(ΔPA) lost the ability to negatively regulate Fzd expression and Wnt/βcatenin signaling (Fig. 2B, C and G). These results suggest that interaction between RNF43 and Fzd, which is indispensable for negative regulation of Wnt/βcatenin signaling, is not essential for suppression of noncanonical Wnt signaling. Moreover, mutants that lack a large part of the C-terminal region in addition to lacking the PA or RING-finger domain (ΔPA;m1 or ΔR;m1) lost the ability to suppress CE movement, indicating the importance of the C-terminal region for negative regulation of noncanonical Wnt signaling (Fig. 6C).

To determine how RNF43 suppresses noncanonical Wnt signaling, we screened proteins for interaction with the C-terminal of RNF43 (RNF43(C)) among the transducer proteins of Wnt signaling pathways. Co-immunoprecipitation experiments revealed that endogenous Dishevelled 2 (Dvl2), known as a regulator in both Wnt/βcatenin signaling and noncanonical Wnt signaling, binds to RNF43(C), although exogenous levels of other transducers including Axin and βcatenin do not (Fig. 7A and not shown). While an established ubiquitin ligase of Dvl, NEDL1, downregulated the expression of Dvl2, RNF43 did not (Fig. 7B). These findings and the results shown in Figure 6 that noncanonical Wnt signal is not regulated by the ubiquitinating activity of RNF43 indicate that RNF43 does not regulate noncanonical Wnt signaling by degradation of Dvl2. Therefore, we examined the manner of the interaction between the C-terminal region of RNF43 and Dvl2. Biochemical analysis showed that Dvl2 lacking

the PDZ domain does not interact with RNF43 (Fig. 7C). In addition, all of the mutants (m1, m7-m8 and m10-m12) lacking the amino acids (478-596) were not able to bind to Dvl2, and partial deletion of PDZ-docking motifs (m17-m19) in this region including class I-III (41) decreased the interaction of RNF43 with Dvl2 (Fig. 7D, E and G). Furthermore, RNF43(m20) mutant lacking the histidine-rich motif (HYHRHRHHHYKK: 549-560 aa.) showed a weak binding to Dvl2, suggesting that interaction of RNF43 with Dvl2 requires the specific structure in RNF43 that is composed of multiple PDZ-docking motifs and a histidine-rich motif.

We next examined whether RNF43-Dvl interaction is essential for the regulation of Fzd expression at the cell surface and for the regulation of Wnt/βcatenin signaling by a flow cytometric analysis and an STF reporter assay. RNF43 deletion mutants lacking the ability to suppress Wnt/βcatenin signaling (m5, m12 and m16) did not downregulate the expression of surface Fzd4 (Fig. 7F-H). Surprisingly, the results obtained from the experiments using RNF43 (m10 and m12) showed that the binding of RNF43 to Dvl2 is not required for downregulation of Fzd4 level and for suppression of Wnt/βcatenin signaling by RNF43, confirming that the regulatory mechanism of noncanonical Wnt signaling by RNF43 is different from that of the Wnt/βcatenin pathway (Fig. 2B, C and G, Fig. 6 and Fig. 7D-H).

It has been reported that the KTXXXW motif in the C-terminal region of Fzd binds to the PDZ domain of Dvl (42, 43). Dvl2 interacted with Fzd5 after Wnt5a stimulation (Fig. 8A). To clarify how RNF43 regulates noncanonical Wnt signaling with Dvl2, we investigated the manner of interactions among RNF43, Dvl2 and Fzd5 after Wnt5a

stimulation. All of these proteins were able to bind to each other, but they did not form a trimeric complex (Fig. 8B). In addition, increasing the amount of RNF43 or RNF43(C) eliminated Fzd5 from Dvl2 through competition in the PDZ domain (Fig. 8C), supporting our results in Figure 6 showing that RNF43 suppresses noncanonical Wnt signaling in Fzd expression-independent but Dvl2 binding-dependent fashions. We also examined the role of RNF43-Dvl2 interactions in suppression of noncanonical Wnt signaling with a series of RNF43 deletion mutants. Wnt5a-induced phosphorylation of Dvl2 was suppressed with RNF43(C and m9) mutants which can bind to Dvl2 as well as with wild-type RNF43 but not with RNF43(m1 and m12) which cannot bind to Dvl2 (Fig. 7D, G and 8D). These results revealed that the interaction of RNF43 with Dvl2 via its cytoplasmic region including a histidine-rich and PDZ binding motifs is indispensable for the suppression of noncanonical Wnt signaling. Moreover, we examined the activity of noncanonical Wnt signaling in tumors, which expressed RNF43 carrying a missense mutation in the extracellular domain (I48T, R127P). These mutants were able to suppress Wnt5a-induced phosphorylation of Dvl2 (Fig. 8E), although both mutants that still retain the ability to interact with Dvl2 induced increase in surface Fzd levels and activation of Wnt/βcatenin signaling (Fig. 3B-E). These findings suggest that the interaction of RNF43(WT and missense mutants) with Dvl2 prevents Wnt5a-dependent binding of Dvl to Fzd, resulting in the inhibition of noncanonical Wnt signaling (Fig. 8E-G).

Regulation of RNF43 expression. Elevated RNF43 expression has been shown in colorectal cancer (CRC) (44) and pancreatic tumor cells (31), and RNF43 is a potential

target of Wnt/βcatenin signaling (28). To investigate how RNF43 expression is regulated, we finally examined RNF43 expression in several cancer cell lines and in normal mouse cells. *RNF43* mRNA was detected in ES cells as well as in several cancer cell lines that contain activating mutations in Wnt/βcatenin signaling (Fig. 9A). To examine whether active Wnt/βcatenin signaling is sufficient to induce RNF43 expression, we stimulated cell lines with Wnt3a CM or CHIR, a specific inhibitor of glycogen synthase kinase 3β (GSK-3β). Expression of RNF43 and its homolog, ZNRF3, was only induced by Wnt stimulation in MEFs or MCF7 cells (Fig. 9B and C). However, RNF43 expression was not induced in ES cells with active Wnt/βcatenin signaling, although *RNF43* mRNA level in ES cells was higher than that in MEFs, suggesting that RNF43 is a potential target of Wnt/βcatenin signaling depending on cellular context and that its expression is differently regulated between stem cells and other cells.

Taken together with our results showing that RNF43 is one of the target genes in active Wnt/βcatenin signaling and that missense mutants of RNF43 increase their protein stability, function as a positive regulator of Wnt/βcatenin signaling and have an ability to suppress noncanonical Wnt signaling, missense mutations in the extracellular domain of RNF43 possibly establish a positive feedback loop of Wnt/βcatenin signaling (Fig. 9D).

DISCUSSION

We showed that missense mutants of RNF43 functions as a positive regulator for Wnt/βcatenin signaling and a negative regulator for noncanonical Wnt signaling, while wild-type RNF43 negatively regulates both Wnt signaling pathways through distinct mechanisms.

In the presence of Wnt1 class or Wnt5a class Wnts, Wnt/βcatenin or noncanonical Wnt signaling is activated to conduct cell behavior. Activation of Wnt/βcatenin signaling leads to the expression of its target genes including RNF43 (27, 28). RNF43 protein is expressed at the cell surface through the ER/Golgi in a normal trafficking pathway, interacts with either Fzd or Dvl and prevents the binding of Dvl to Fzd. Interaction of the extracellular PA domain of RNF43 with the CRD of Fzd induces ubiquitination of Fzd by its RING-finger domain and causes the endocytosis of Fzd and RNF43 in order to downregulate surface expression of Fzd, followed by the termination of both Wnt/βcatenin and noncanonical Wnt signaling. The elimination of Dvl2 from Fzd may play a role in the suppression of noncanonical Wnt signaling. However, this suppressive activity may be not prominent in the regulation of noncanonical Wnt signaling with WT RNF43, because it acts at the more downstream event of downregulation of Fzd.

It has been reported that loss of functional mutants of RNF43 does not express at the cell surface (31). In this study, we showed that mutant RNF43 accumulates at the ER (see Fig. 4 and 5). Lack of surface RNF43 abrogates the internalization of Fzd

resulting in the Rspo-independent accumulation of Fzd at the cell surface and the aberrant activation of Wnt/βcatenin signaling. Missense mutations of RNF43 which lead to the accumulation of them in the ER impair normal intracellular trafficking of RNF43 from the ER to the lysosome through the cell surface and the endosome, resulting in the stabilization of mutant RNF43. On the other hand, noncanonical Wnt signaling is still suppressed in the presence of mutant RNF43 with Dvl2 at the ER, although Fzd is accumulated at the cell surface. Noncanonical Wnt signaling may be suppressed by mutant RNF43 due to the elimination of Dvl from surface Fzd and/or due to the capture of Dvl2 by mutant RNF43 in the ER through the interaction between the PDZ of Dvl and the cytoplasmic region of RNF43.

We showed that N-terminal portion of RNF43 including the extracellular PA domain and the intracellular RING-finger domain (1-317 aa) is required for inhibition of Fzd expression and Wnt/βcatenin signaling but not for suppression of noncanonical Wnt signaling. In contrast, a part of the C-terminal region including PDZ-binding motifs and a histidine-rich motif (318-783 aa) is indispensable for Dvl2-dependent suppression of noncanonical Wnt signaling but is not essential for the regulation of Wnt/βcatenin signaling, suggesting distinct roles of Dvl2 in Wnt/βcatenin and noncanonical Wnt signaling (Fig. 9D, left). However, it is still unclear whether other unidentified regulators function to suppress Wnt/βcatenin signaling with the C-terminal region of RNF43 because some deletion mutants (m5, m12 and m16) facilitated Wnt/βcatenin signaling without the upregulation of Fzd. Hence, it is important to perform further structural analysis to determine the role and importance of RNF43-Dvl2

binding in noncanonical Wnt signaling and to identify the proteins that interact with the C-terminal region to modulate Wnt/βcatenin signaling.

RNF43 mutants carrying missense mutations in their extracellular domains increased the surface expression of Fzd and Wnt/βcatenin signaling, suggesting that mutant RNF43 can act as a dominant negative mutant because of its ability to interact with Fzd. However, these mutants did not interact with Fzd in cells due to their mislocalization. RNF43(ΔPA) mutant lacking the ability to bind to Fzd was not able to accumulate Fzd at the cell surface and did not exhibit a dominant negative effect in the regulation of Wnt/βcatenin signaling. Our results suggested that the dominant negative effect of missense mutants in the regulation of Fzd expression is not caused by the interaction of RNF43 with Fzd but possibly by the inhibition of endogenous ZNRF3 by an unelucidated mechanism because these mutants still retain the ability to facilitate Wnt/βcatenin signaling even in RNF43 knock-down cells. The effect of mislocalization of mutant RNF43 in the regulation of Wnt signaling pathways has not been fully elucidated. However, it has recently been reported that an aberrant localization of the receptor protein Kit in the ER leads to the activation of oncogenic downstream signaling due to abnormal trafficking originating from its missense mutation, and the mechanism shown in that report may be similar to the mechanism of activation of Wnt/βcatenin signaling by RNF43 mutants (45).

Others have shown that *RNF43* and its homolog *ZNRF3* are potential target genes of Wnt/βcatenin signaling for suppression of Fzd expression at the cell surface to attenuate Wnt/βcatenin signaling and form a negative-feedback loop (27, 28). Our

results lead us to speculate that missense mutations of RNF43 identified in patients with tumors cause the facilitation of Wnt/βcatenin signaling and further expression of mutant RNF43, thereby missense mutants of RNF43 act as positive regulators of Wnt/βcatenin signaling, resulting in the formation of a positive-feedback loop and tumorigenesis with other factors including active-Ras (33). In addition, these mutants still retain the inhibitory function for noncanonical Wnt signaling due to the presence of the C-terminal region at which Dvl2 binds, resulting in further suppression of noncanonical Wnt signaling and a decline of the suppressive ability for Wnt/βcatenin signaling through an NLK- and/or Siah-dependent pathway and in acceleration of tumorigenesis (Fig. 9D, right).

It is still controversial that wild-type RNF43 is highly expressed in ES cells, which require activation of Wnt/βcatenin signaling to maintain their pluripotency (46). Nevertheless, our results showed that there is a higher expression of RNF43 in ES cells than in MEFs and that RNF43 suppresses noncanonical Wnt signaling. Furthermore, these observations are inconsistent with the result of a previous study showing that a switching process from noncanonical Wnt signaling to Wnt/βcatenin signaling is required for the proliferation of hematopoietic stem cells (HSCs) (47). These inconsistent results suggest that RNF43 expression is differently regulated in stem cells from in other types of cells and that RNF43 does not suppress Wnt/βcatenin signaling via Fzd expression but plays distinct roles in ES sells with other partners to maintain the "stemness". On the other hand, the activation of Wnt/βcatenin signaling and the suppression of noncanonical Wnt signaling by missense mutations of RNF43 can

explain why these mutations were found in the patient with tumors because both of these effects originating from mutations of RNF43 can switch from noncanonical Wnt signals to Wnt/βcatenin signaling and may turn the quiescent stem cells out of niche to induce their proliferation.

A recent study also showed that inactivating mutations of *RNF43* confer Wnt dependency in pancreatic tumors (31). In addition, several reports (33, 34, 48, 49) and the COSMIC database have shown that somatic mutations in the RNF43 locus were also identified in tumor samples from the skin, ovary, breast, prostate, liver, pancreas and large intestine, suggesting that RNF43 functions as a tumor suppressor in many tissues.

In conclusion, RNF43 may play a critical role not only in maintenance of stem cells but also in tumorigenesis, and it may be an appropriate molecular target for cancer diagnosis or therapy through its extracellular interaction with related molecules such as Fzd.

Acknowledgements

We thank Yuri Soida and Miho Uchiumi for administrative assistance and Mai Yaegashi and Misumi Matsuo for technical assistance. We also thank Toshio Kitamura, Akira Kikuchi, Masa-aki Nakaya and Mutsuo Furihata for providing materials and Hajime Sasaki for data analysis.

This work was supported by KAKENHI (to S.H.; 24112006, 24390065 and to T.T.; 25430102) from the Ministry of Education, Culture, Sports, Science and Technology in Japan.

References

1. **Yamaguchi TP.** 2001. Heads or tails: Wnts and anterior-posterior patterning. Curr. Biol. **11:**R713-724.
2. **Logan CY, Nusse R.** 2004. The Wnt signaling pathway in development and disease. Annu. Rev. Cell Dev. Biol. **20:**781-810.
3. **Moon RT, Kohn AD, De Ferrari GV, Kaykas A.** 2004. WNT and beta-catenin signalling: diseases and therapies. Nat. Rev. Genet. **5:**691-701.
4. **MacDonald BT, Tamai K, He X.** 2009. Wnt/beta-catenin signaling: components, mechanisms, and diseases. Dev. Cell **17:**9-26.
5. **Kikuchi A, Yamamoto H, Sato A, Matsumoto S.** 2012. Wnt5a: its signalling, functions and implication in diseases. Acta Physiol. **204:**17-33.
6. **Clevers H, Nusse R.** 2012. Wnt/beta-catenin signaling and disease. Cell **149:**1192-1205.
7. **Kikuchi A, Yamamoto H, Sato A.** 2009. Selective activation mechanisms of Wnt signaling pathways. Trends Cell Biol **19:**119-129.
8. **Torres MA, Yang-Snyder JA, Purcell SM, DeMarais AA, McGrew LL, Moon RT.** 1996. Activities of the Wnt-1 class of secreted signaling factors are antagonized by the Wnt-5A class and by a dominant negative cadherin in early Xenopus development. J. Cell Biol. **133:**1123-1137.
9. **Kitagawa M, Hatakeyama S, Shirane M, Matsumoto M, Ishida N, Hattori K, Nakamichi I, Kikuchi A, Nakayama K.** 1999. An F-box protein, FWD1, mediates ubiquitin-dependent proteolysis of beta-catenin. EMBO J. **18:**2401-2410.
10. **Roose J, Molenaar M, Peterson J, Hurenkamp J, Brantjes H, Moerer P, van de Wetering M, Destree O, Clevers H.** 1998. The Xenopus Wnt effector XTcf-3 interacts with Groucho-related transcriptional repressors. Nature **395:**608-612.
11. **Yamaguchi TP, Bradley A, McMahon AP, Jones S.** 1999. A Wnt5a pathway underlies outgrowth of multiple structures in the vertebrate embryo. Development **126:**1211-1223.
12. **Mikels AJ, Nusse R.** 2006. Purified Wnt5a protein activates or inhibits

beta-catenin-TCF signaling depending on receptor context. PLoS Biol. **4:**e115.

13. **Liu J, Stevens J, Rote CA, Yost HJ, Hu Y, Neufeld KL, White RL, Matsunami N.** 2001. Siah-1 mediates a novel beta-catenin degradation pathway linking p53 to the adenomatous polyposis coli protein. Mol. Cell **7:**927-936.
14. **Matsuzawa SI, Reed JC.** 2001. Siah-1, SIP, and Ebi collaborate in a novel pathway for beta-catenin degradation linked to p53 responses. Mol. Cell **7:**915-926.
15. **Topol L, Jiang X, Choi H, Garrett-Beal L, Carolan PJ, Yang Y.** 2003. Wnt-5a inhibits the canonical Wnt pathway by promoting GSK-3-independent beta-catenin degradation. Journal of Cell Biology **162:**899-908.
16. **Ishitani T, Ninomiya-Tsuji J, Nagai S, Nishita M, Meneghini M, Barker N, Waterman M, Bowerman B, Clevers H, Shibuya H, Matsumoto K.** 1999. The TAK1-NLK-MAPK-related pathway antagonizes signalling between beta-catenin and transcription factor TCF. Nature **399:**798-802.
17. **Ishitani T, Kishida S, Hyodo-Miura J, Ueno N, Yasuda J, Waterman M, Shibuya H, Moon RT, Ninomiya-Tsuji J, Matsumoto K.** 2003. The TAK1-NLK mitogen-activated protein kinase cascade functions in the Wnt-5a/Ca(2+) pathway to antagonize Wnt/beta-catenin signaling. Mol. Cell Biol. **23:**131-139.
18. **Polakis P.** 2007. The many ways of Wnt in cancer. Curr. Opin. Genet. Dev. **17:**45-51.
19. **Tauriello DV, Maurice MM.** 2010. The various roles of ubiquitin in Wnt pathway regulation. Cell Cycle **9:**3700-3709.
20. **Mukai A, Yamamoto-Hino M, Awano W, Watanabe W, Komada M, Goto S.** 2010. Balanced ubiquitylation and deubiquitylation of Frizzled regulate cellular responsiveness to Wg/Wnt. EMBO J. **29:**2114-2125.
21. **Miyazaki K, Fujita T, Ozaki T, Kato C, Kurose Y, Sakamoto M, Kato S, Goto T, Itoyama Y, Aoki M, Nakagawara A.** 2004. NEDL1, a novel ubiquitin-protein isopeptide ligase for dishevelled-1, targets mutant superoxide dismutase-1. J. Biol. Chem. **279:**11327-11335.
22. **Simons M, Gloy J, Ganner A, Bullerkotte A, Bashkurov M, Kronig C, Schermer B, Benzing T, Cabello OA, Jenny A, Mlodzik M, Polok B, Driever W, Obara T, Walz G.** 2005. Inversin, the gene product mutated in

nephronophthisis type II, functions as a molecular switch between Wnt signaling pathways. Nat. Genet. **37:**537-543.

23. **Tauriello DV, Haegebarth A, Kuper I, Edelmann MJ, Henraat M, Canninga-van Dijk MR, Kessler BM, Clevers H, Maurice MM.** 2010. Loss of the tumor suppressor CYLD enhances Wnt/beta-catenin signaling through K63-linked ubiquitination of Dvl. Mol. Cell **37:**607-619.
24. **Zhang Y, Liu S, Mickanin C, Feng Y, Charlat O, Michaud GA, Schirle M, Shi X, Hild M, Bauer A, Myer VE, Finan PM, Porter JA, Huang SM, Cong F.** 2011. RNF146 is a poly(ADP-ribose)-directed E3 ligase that regulates axin degradation and Wnt signalling. Nat. Cell Biol. **13:**623-629.
25. **Callow MG, Tran H, Phu L, Lau T, Lee J, Sandoval WN, Liu PS, Bheddah S, Tao J, Lill JR, Hongo JA, Davis D, Kirkpatrick DS, Polakis P, Costa M.** 2011. Ubiquitin ligase RNF146 regulates tankyrase and Axin to promote Wnt signaling. PLoS ONE **6:**e22595.
26. **Choi J, Park SY, Costantini F, Jho EH, Joo CK.** 2004. Adenomatous polyposis coli is down-regulated by the ubiquitin-proteasome pathway in a process facilitated by Axin. J. Biol. Chem. **279:**49188-49198.
27. **Hao HX, Xie Y, Zhang Y, Charlat O, Oster E, Avello M, Lei H, Mickanin C, Liu D, Ruffner H, Mao X, Ma Q, Zamponi R, Bouwmeester T, Finan PM, Kirschner MW, Porter JA, Serluca FC, Cong F.** 2012. ZNRF3 promotes Wnt receptor turnover in an R-spondin-sensitive manner. Nature **485:**195-200.
28. **Koo BK, Spit M, Jordens I, Low TY, Stange DE, van de Wetering M, van Es JH, Mohammed S, Heck AJ, Maurice MM, Clevers H.** 2012. Tumour suppressor RNF43 is a stem-cell E3 ligase that induces endocytosis of Wnt receptors. Nature **488:**665-669.
29. **Shinada K, Tsukiyama T, Sho T, Okumura F, Asaka M, Hatakeyama S.** 2011. RNF43 interacts with NEDL1 and regulates p53-mediated transcription. Biochem. Biophys. Res. Commun. **404:**143-147.
30. **Morita S, Kojima T, Kitamura T.** 2000. Plat-E: an efficient and stable system for transient packaging of retroviruses. Gene Ther. **7:**1063-1066.
31. **Jiang X, Hao HX, Growney JD, Woolfenden S, Bottiglio C, Ng N, Lu B, Hsieh MH, Bagdasarian L, Meyer R, Smith TR, Avello M, Charlat O, Xie Y, Porter JA, Pan S, Liu J, McLaughlin ME, Cong F.** 2013. Inactivating

mutations of RNF43 confer Wnt dependency in pancreatic ductal adenocarcinoma. Proc. Natl. Acad. Sci. USA **110:**12649-12654.

32. **Matsuda M, Tsukiyama T, Bohgaki M, Nonomura K, Hatakeyama S.** 2007. Establishment of a newly improved detection system for NF-kappaB activity. Immunol. Lett. **109:**175-181.

33. **Wu J, Jiao Y, Dal Molin M, Maitra A, de Wilde RF, Wood LD, Eshleman JR, Goggins MG, Wolfgang CL, Canto MI, Schulick RD, Edil BH, Choti MA, Adsay V, Klimstra DS, Offerhaus GJ, Klein AP, Kopelovich L, Carter H, Karchin R, Allen PJ, Schmidt CM, Naito Y, Diaz LA, Jr., Kinzler KW, Papadopoulos N, Hruban RH, Vogelstein B.** 2011. Whole-exome sequencing of neoplastic cysts of the pancreas reveals recurrent mutations in components of ubiquitin-dependent pathways. Proc. Natl. Acad. Sci. USA **108:**21188-21193.

34. **Ong CK, Subimerb C, Pairojkul C, Wongkham S, Cutcutache I, Yu W, McPherson JR, Allen GE, Ng CC, Wong BH, Myint SS, Rajasegaran V, Heng HL, Gan A, Zang ZJ, Wu Y, Wu J, Lee MH, Huang D, Ong P, Chan-on W, Cao Y, Qian CN, Lim KH, Ooi A, Dykema K, Furge K, Kukongviriyapan V, Sripa B, Wongkham C, Yongvanit P, Futreal PA, Bhudhisawasdi V, Rozen S, Tan P, Teh BT.** 2012. Exome sequencing of liver fluke-associated cholangiocarcinoma. Nat. Genet. **44:**690-693.

35. **Chen PH, Chen X, Lin Z, Fang D, He X.** 2013. The structural basis of R-spondin recognition by LGR5 and RNF43. Genes Dev. **27:**1345-1350.

36. **He X, Saint-Jeannet JP, Wang Y, Nathans J, Dawid I, Varmus H.** 1997. A member of the Frizzled protein family mediating axis induction by Wnt-5A. Science **275:**1652-1654.

37. **van Amerongen R, Fuerer C, Mizutani M, Nusse R.** 2012. Wnt5a can both activate and repress Wnt/beta-catenin signaling during mouse embryonic development. Dev Biol **369:**101-114.

38. **Grossmann AH, Yoo JH, Clancy J, Sorensen LK, Sedgwick A, Tong Z, Ostanin K, Rogers A, Grossmann KF, Tripp SR, Thomas KR, D'Souza-Schorey C, Odelberg SJ, Li DY.** 2013. The small GTPase ARF6 stimulates beta-catenin transcriptional activity during WNT5A-mediated melanoma invasion and metastasis. Sci. Signal **6:**ra14.

39. **de Lau W, Peng WC, Gros P, Clevers H.** 2014. The R-spondin/Lgr5/Rnf43

module: regulator of Wnt signal strength. Genes & Development **28:**305-316.

40. **Glinka A, Dolde C, Kirsch N, Huang YL, Kazanskaya O, Ingelfinger D, Boutros M, Cruciat CM, Niehrs C.** 2011. LGR4 and LGR5 are R-spondin receptors mediating Wnt/-catenin and Wnt/PCP signalling. EMBO Rep. **12:**1055-1061.
41. **Lee HJ, Zheng JJ.** 2010. PDZ domains and their binding partners: structure, specificity, and modification. Cell Commun. Signal **8:**8.
42. **Wong HC, Bourdelas A, Krauss A, Lee HJ, Shao Y, Wu D, Mlodzik M, Shi DL, Zheng J.** 2003. Direct binding of the PDZ domain of Dishevelled to a conserved internal sequence in the C-terminal region of Frizzled. Mol. Cell **12:**1251-1260.
43. **Punchihewa C, Ferreira AM, Cassell R, Rodrigues P, Fujii N.** 2009. Sequence requirement and subtype specificity in the high-affinity interaction between human frizzled and dishevelled proteins. Protein Sci. **18:**994-1002.
44. **Yagyu R, Furukawa Y, Lin YM, Shimokawa T, Yamamura T, Nakamura Y.** 2004. A novel oncoprotein RNF43 functions in an autocrine manner in colorectal cancer. Int. J. Oncol. **25:**1343-1348.
45. **Obata Y, Toyoshima S, Wakamatsu E, Suzuki S, Ogawa S, Esumi H, Abe R.** 2014. Oncogenic Kit signals on endolysosomes and endoplasmic reticulum are essential for neoplastic mast cell proliferation. Nat. Commun. **5:**5715.
46. **Holland JD, Klaus A, Garratt AN, Birchmeier W.** 2013. Wnt signaling in stem and cancer stem cells. Curr. Opin. Cell Biol. **25:**254-264.
47. **Sugimura R, He XC, Venkatraman A, Arai F, Box A, Semerad C, Haug JS, Peng L, Zhong XB, Suda T, Li L.** 2012. Noncanonical Wnt signaling maintains hematopoietic stem cells in the niche. Cell **150:**351-365.
48. **Ryland GL, Hunter SM, Doyle MA, Rowley SM, Christie M, Allan PE, Bowtell DD, Gorringe KL, Campbell IG.** 2013. RNF43 is a tumour suppressor gene mutated in mucinous tumours of the ovary. J. Pathol. **229:**469-476.
49. **Xing C, Zhou W, Ding S, Xie H, Zhang W, Yang Z, Wei B, Chen K, Su R, Cheng J, Zheng S, Zhou L.** 2013. Reversing effect of ring finger protein 43 inhibition on malignant phenotypes of human hepatocellular carcinoma. Mol. Cancer Ther. **12:**94-103.

FIGURE LEGENDS

Fig. 1. Finding of putative ubiquitin ligases that specifically regulate Wnt/βcatenin signaling. (A, B) A series of plasmids that express RING-finger proteins (RNFs) and tripartite motif proteins (TRIMs) (expression confirmed; not shown) was transfected without (A) or with (B) a Wnt3a expression plasmid into STF293 cells. Luciferase activities were then measured to identify the regulator in Wnt/βcatenin signaling. (C, D) Increasing amounts of the RNF43 were co-expressed with Wnt3a or Wnt1 in STF293 cells to examine the activity of Wnt/βcatenin signaling(C). RNF43-transfected STF293 cells were stimulated with Wnt3a-conditioned media (CM) for luciferase assays (D). Asterisks indicate a significant difference ($P < .05$, Student's *t*-test) from Wnt3a- or Wnt1-stimulated control cells (C) or from Wnt3a-stimulated control cells (D). (E) RNF43 was expressed in HEK293 cells with Notch reporter and Notch intra-cellular domain (NICD) for dual-luciferase assay. (F) RNF43 was co-transfected in HeLa cells with cNAT-EGFP:Luc2 reporter plasmids, and these cells were then stimulated with rTNFα protein for dual-luciferase assay. (G) mRNA was injected into the ventral side of *Xenopus* embryos and xWnt8a-induced axis duplication was evaluated to examine the function of RNF43 *in vivo*. See also Table 1. The injection site of mRNA is illustrated (upper). Scale bars = 1 mm. (H) The role of RING-finger domain of RNF43 in regulation of the expression level of endogenous Fzd4 on the cell surface was confirmed by flowcytometric analysis with RNF43 and RNF43(ΔR) mutant in HEK293 cells.

Fig. 2 Extracellular interaction of RNF43 with Fzd5 is essential for the suppression of Wnt/βcatenin signaling. (A) Positions of somatic mutations identified by whole-exome sequencing with pancreatic tumors and cholangiocarcinomas from patients in previous studies are illustrated. Missense mutations were frequently observed in the extracellular PA domain in both tumors. Arrows and arrowheads indicate nonsense and missense mutations, respectively. PA, protease-associated domain; TM, transmembrane motif; RING, RING-finger domain. (B) The role of the extracellular PA domain of RNF43 in Wnt/βcatenin signaling was examined by luciferase reporter assays. RNF43 mutant constructs are illustrated at the top. Asterisks indicate a significant difference ($P < .05$, Student's *t*-test) from Wnt3a-stimulated control cells. (C) Surface expression of endogenous Fzd4 in RNF43- and RNF43(ΔPA)-expressing HEK293 cells was investigated by flow cytometry. NS, not stained; NC, negative control (empty vector-transfected). (D, E) The role of CRD (D) and PA (E) domains in RNF43-Fzd5 interaction were examined by co-immunoprecipitation. Fzd5 and RNF43 mutant constructs are illustrated at the top of each figure. CRD, cysteine-rich domain; CPD, cytoplasmic domain. (F) The secreted form of the PA domain of RNF43 and CRD of Fzd5 (sPA, sCRD) were expressed in HEK293T cells. sCRD was immunoprecipitated from the cell lysates or the culture supernatant to detect its binding to sPA. RNF43 and Fzd5 mutant constructs are illustrated at the top. (G) mRNA was injected into *Xenopus* embryos and head formation was evaluated (middle). Quantitative results are shown (lower). The injection site and RNF43 mutants are illustrated (upper). Scale bars = 1

mm. Asterisks indicate a significant difference ($P < .05$, ANOVA) from RNF43-injected embryos.

Fig. 3 Mutations of RNF43 identified in patients with tumors invert the function of RNF43 in regulation of Wnt/βcatenin signaling. (A) Missense mutations in the extracellular domain of RNF43 tumor suppressor are illustrated. Mutations that change the function of RNF43 from a negative regulator to a positive regulator in Wnt/βcatenin signaling shown in B are indicated in red. (B) The effects of the mutations in Wnt/βcatenin signaling were examined in STF293 cells. Expression levels of RNF43 mutants are shown at the bottom. RNF43 mutants that facilitate (more than x2-fold) Wnt/βcatenin signaling compared to Wnt3a-stimulated control cells are indicated in red. (C) Endogenous RNF43 was knocked down with siRNA and then missense mutants of RNF43 resistant to siRNA (RNF43(siR)) were restored to clarify the role of mutations in STF293 cells stably expressing these mutants. (D) RNF43 mutants that enhance the Wnt/βcatenin signaling were examined by flow cytometry for their ability to regulate endogenous Fzd4 expression at the surface of HEK293 cells. NS, not stained; NC, negative control. (E) mRNAs of RNF43 mutants and/or xWnt8 (low dose) were injected with the indicated combinations into *Xenopus* embryos as illustrated (upper) to confirm the effects of missense mutations in Wnt/βcatenin and noncanonical Wnt signaling. See also Table 1. Scale bars = 1 mm. (F) RNF43 and its derivatives were expressed in STF293 cells, and the cells were then stimulated with Wnt3a or Wnt5a CM to evaluate the activity of Wnt/βcatenin signaling by a luciferase assay (right). Accumulation of

active-βcatenin was also examined in these stimulated cells (left).

Fig. 4 Mutations in the extracellular domain of RNF43 change the localization of both RNF43 and Fzd5. (A) Interactions between RNF43 missense mutants and Fzd5 were examined in HEK293 cells by co-immunoprecipitation. (B) RNF43 and its mutants were expressed in HEK293T cells. Cells were homogenized and then fractioned by centrifugation. Membrane, M; nuclear, N; cytoplasm, C. (C) RNF43(WT, I48T, L82S, R127P)-EGFP were expressed in HeLa cells and then subcellular localization of RNF43 was observed by a fluorescence microscope. (D) HA-tagged RNF43 and its mutants were expressed with FLAG-tagged Fzd5 in HeLa cells. Subcellular localization of RNF43 and Fzd5 was observed by a fluorescence microscope. (E) EGFP-tagged RNF43 and its mutant were expressed with DsRed-tagged Fzd5 in HeLa cells. Subcellular localization of RNF43 and Fzd5 was observed by a fluorescence microscope (upper) and the number of cells showing co-localization was quantified (bottom). (F) RNF43-EGFP was expressed with DsRed2- or TdTomato-tagged organelle markers (ER, endoplasmic reticulum; Rab5, early endosome; Rab7, late endosome; Rab11, recycling endosome) in HeLa cells, and then subcellular localization of RNF43 was observed by a fluorescence microscope. (G) RNF43(WT and R127P)-EGFP were expressed with DsRed2- or TdTomato-tagged organelle markers in HeLa cells to observe the subcellular localization of RNF43. (F, G) The intensity of signals on the thin white line indicated in the images is shown on the right side. Arrows indicate the co-localization of RNF43 with organelle markers. (E, G) The percentages of

co-localization of RNF43 with organelle markers are shown (bottom). (C-G) White bars = 20 μm. (E, G) Asterisks indicate significant differences ($P < .05$, ANOVA) from RNF43(WT) cells.

Fig. 5 Evidence of ER localization of RNF43 mutants (A) NIH3T3 cells stably expressing RNF43 or its derivatives were treated with CHX for the indicated times, and then expression of RNF43 proteins was examined by immunoblotting. Relative expression levels of RNF43 normalized by GAPDH are shown at the bottom. (B) The protein levels of RNF43 and ubiquitinated RNF43 were examined with MG132 treatment by immunoblotting. Relative expression and ubiquitination levels of RNF43 normalized by GAPDH are shown in the middle and at the bottom, respectively. Their relative levels of them in each MG132 (-) cell line are defined as 1. (C) Interactions between RNF43 mutants and Rspo1 were examined in HEK293 cells by co-immunoprecipitation. (D) RNF43 and its mutants were expressed in STF293 cells and then cells were stimulated with Wnt3a CM and Rspo1. The responsiveness of RNF43 to Rspo1 was examined by luciferase reporter assay. The relative levels of luciferase activities in the absence of Rspo1 are defined as 1. (E) STF293 cells stably expressing RNF43 mutants were examined by FACS analysis with anti-Lgr5 mAbs (middle and right) and luciferase assay with Wnt3a CM to show the activation of Wnt/βcatenin signaling via Fzds accumulation (left). The relative levels of luciferase activity or surface Lgr5 expression in mock cells are defined as 1.

Fig. 6 The C-terminal region of RNF43 is required for the suppression of noncanonical Wnt signaling. (A) Animal cap elongation assays were performed with activin and *RNF43* or *RNF43*(Δ*R*) mRNA to examine the function of RNF43 in CE movements (right) as illustrated (upper left). RNF43 mutant constructs examined are shown in the left middle part. The results of the animal cap assay are depicted graphically (lower left). (B) The ability of RNF43 mutants to modulate Wnt5a-induced Dvl2 phosphorylation was examined in RNF43 stably-expressing NIH3T3 (upper) and in expression vectors-transfected HEK293 cells (lower). The graphs on the right show the relative levels of Dvl2 phosphorylation normalized to total Dvl2 (NIH3T3) or GAPDH (HEK293T). (C) The roles of the PA domain, the RING-finger domain and the C-terminal region of RNF43 in noncanonical Wnt signaling were investigated in animal cap elongation assays with RNF43 mutants (ΔPA, ΔPA;m1, ΔR;m1) (right). RNF43 mutant constructs examined are illustrated in the upper left part. The effects of RNF43 mutants on animal cap elongation are summarized graphically (lower left). (A, C) Scale bars = 1 mm. Asterisks indicate a significant difference ($P < .05$, ANOVA) from LacZ-injected, activin-treated control embryos (A) or RNF43-injected, activin-treated embryos (C).

Fig. 7 Interaction of RNF43 with Dvl2 is not required for inhibition of Wnt/βcatenin signaling. (A) Interaction between RNF43 and endogenous Dvl2 was examined with RNF43(C) mutant in HEK293 cells by immunoprecipitation. (B) Dvl2 was co-expressed with RNF43 or NEDL1 in HEK293T cells, and then the cells were treated

with CHX for the indicated times to examine the stability of Dvl2 proteins by immunoblotting. (C) RNF43(WT and m13) were co-transfected with Dvl2(WT and ΔPDZ) into HEK293T cells, and then the interactions between Dvl2 and RNF43 was examined by immunoprecipitation. (D) A series of RNF43 deletion mutants shown in G were co-transfected with Dvl2 to HEK293T cells, and then the interactions between Dvl2 and RNF43 mutants were examined by immunoprecipitation. (E) Amino acid sequence of RNF43(478-596). A histidine-rich motif of RNF43 is shown as blue bold letters. Consensus sequences known as PDZ-interacting motifs are indicated as red, green or underlined letters. ϕ: hydrophobic amino acids. (F) STF-reporter assays using a series of RNF43 mutants to examine the relationship between the suppressive activity of RNF43 and its ability to interact with Dvl2. Asterisks indicate a significant difference from Wnt3a-stimulated control cells. (G) The RNF43 deletion mutants used in D and F are illustrated on the left. The abilities to interact with Dvl2 and to suppress Wnt/βcatenin signaling are summarized. Red box; the region essential for the binding to Dvl2. (H) RNF43 mutants were examined by flow cytometry for their ability to regulate endogenous Fzd4 expression on the surface of HEK293 cells. NS, not stained; NC, negative control.

Fig. 8 Interaction of RNF43 with Dvl2 is indispensable for suppression of noncanonical Wnt signaling. (A) Dvl2 was co-transfected with Fzd5 to HEK293 cells, and then time-dependent interaction between Dvl2 and Fzd5 after Wnt3a or Wnt5a stimulation was examined by immunoprecipitation. (B, C) The indicated expression vectors were

transfected into HEK293T cells, and then the cells were stimulated with Wnt5a CM for 60 min and lysed for immunoprecipitation to examine the interaction of Fzd5 with RNF43 and Dvl2 (B) or of Dvl2 with Fzd and increasing amount of RNF43 (C). (D, E) HEK293 cells expressing RNF43 deletion mutants (D) or expressing missense mutants (E) were stimulated with rWnt5a for the indicated times, and then examined the phosphorylation level of Dvl2 by immunoblotting. Relative phosphorylation levels of Dvl2 normalized by GAPDH are shown on the left. P-Dvl2, phospho-Dvl2. (F) RNF43 missense mutants were expressed with Dvl2 to HEK293T cells, and interactions between Dvl2 and RNF43 were then examined by immunoprecipitation. (G) HA-tagged RNF43 and its mutant were transfected with EGFP-tagged Dvl2 into HeLa cells. The subcellular localization of Dvl2 and RNF43 was observed by a fluorescence microscope. White bars = 20 μm.

Fig. 9 *RNF43* is a potential target gene of Wnt/βcatenin signaling in a manner dependent on the cellular context. (A) The mRNA expression of *RNF43* and its homolog *ZNRF3* were examined by RTPCR using several murine and human cell lines. (B) Cell lines were treated with 3 μM CHIR or Wnt3a CM for 24 h to activate Wnt/βcatenin signaling. The levels of *RNF43* and *ZNRF3* mRNA were examined by RTPCR. (C) Induction of *RNF43* and *ZNRF3* in B was confirmed by quantitative real-time PCR. All of the relative levels of RNF43 and ZNRF3 to non-stimulated (NC) cells were defined as 1 in each cell line. (D) Schematic diagram for regulation of the Wnt signaling pathway and tumorigenesis by WT and mutant RNF43. WT RNF43

functions as a negative regulator of both Wnt/βcatenin signaling and noncanonical Wnt signaling. Induction of WT RNF43 by active Wnt/βcatenin signaling induces WT RNF43 expression and establishes a negative feedback loop to terminate the activation of Wnt/βcatenin signaling and suppress tumorigenesis. In contrast, missense mutants of RNF43 are more stable than the wild type and function as positive regulators of Wnt/βcatenin signaling. Mutant RNF43 retains the ability to suppress noncanonical Wnt signaling, which can negatively regulate Wnt/βcatenin signaling. Activation of Wnt/βcatenin signaling by these effects of mutant RNF43 induces further expression of itself, resulting in the establishment of a positive feedback loop and facilitation of tumorigenesis.

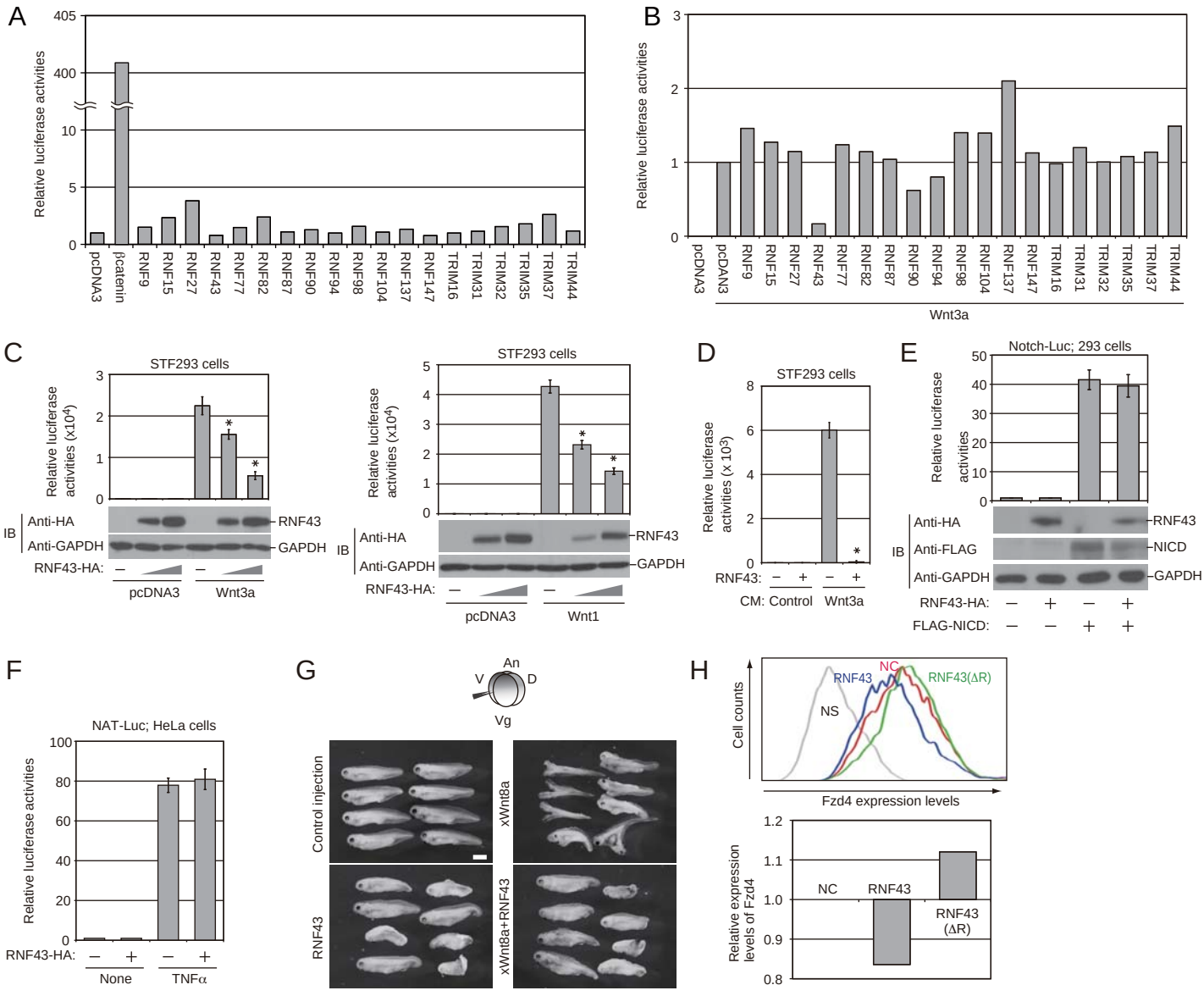

Tsukiyama_Figure1

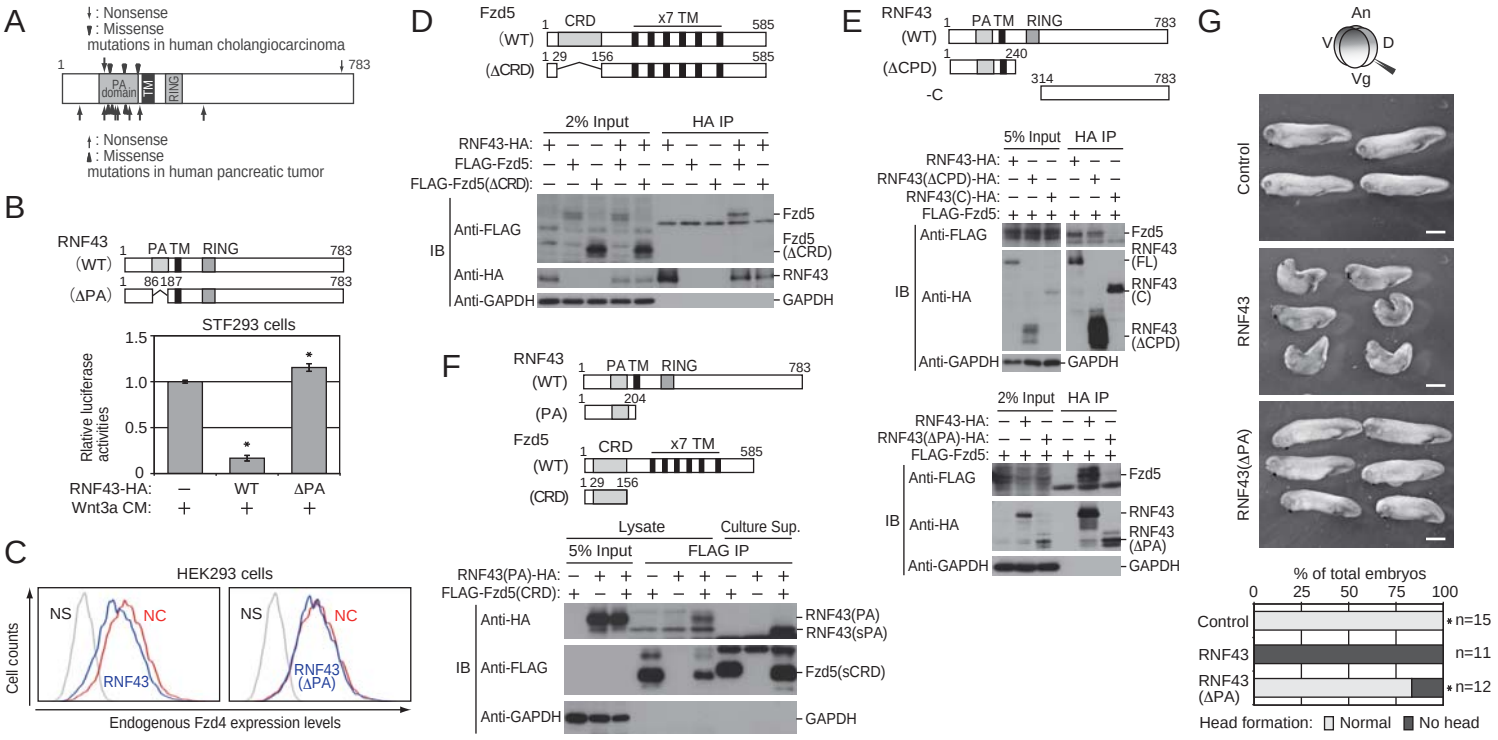

Tsukiyama_Figure2

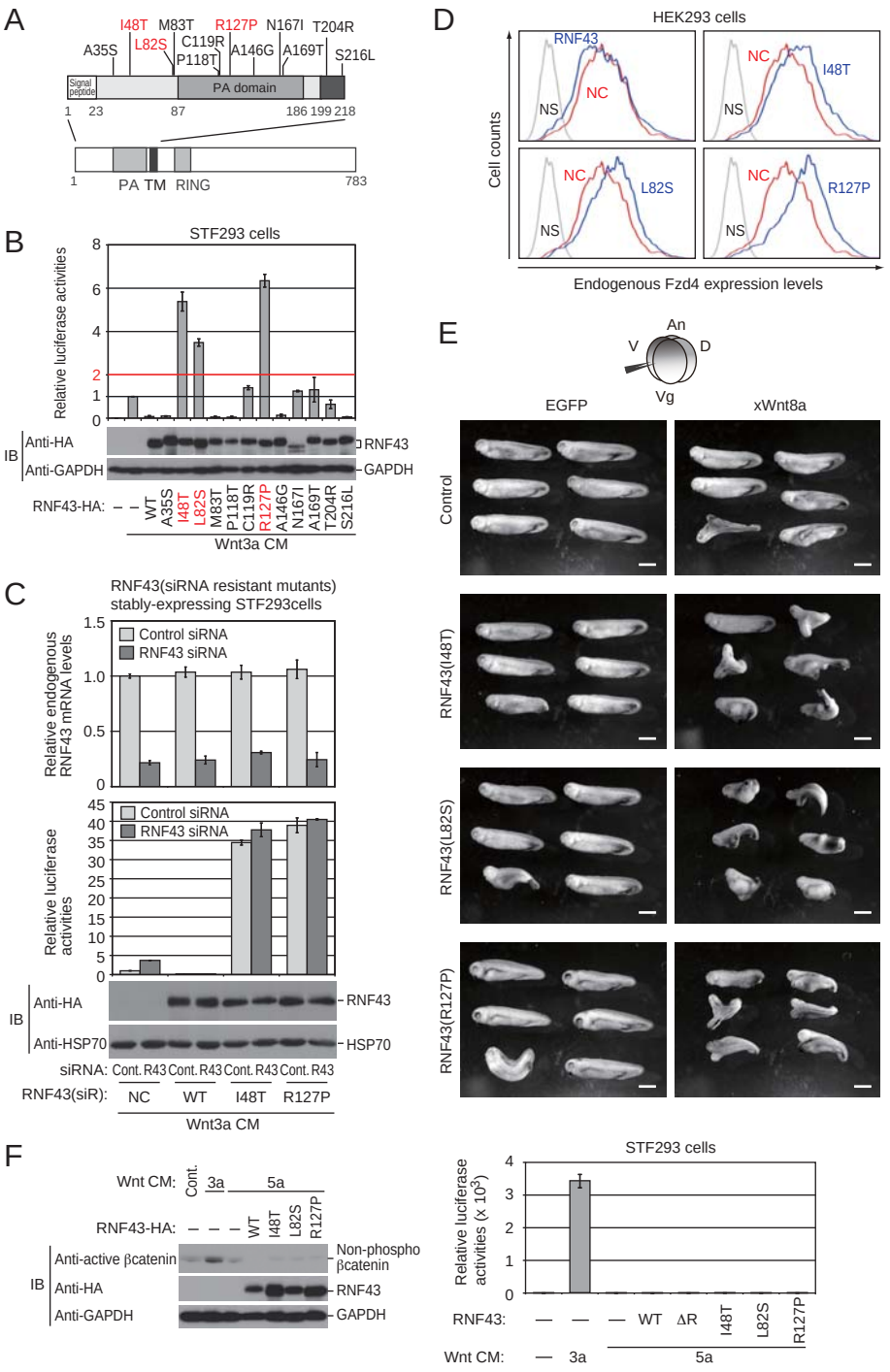

Tsukiyama_Figure 3

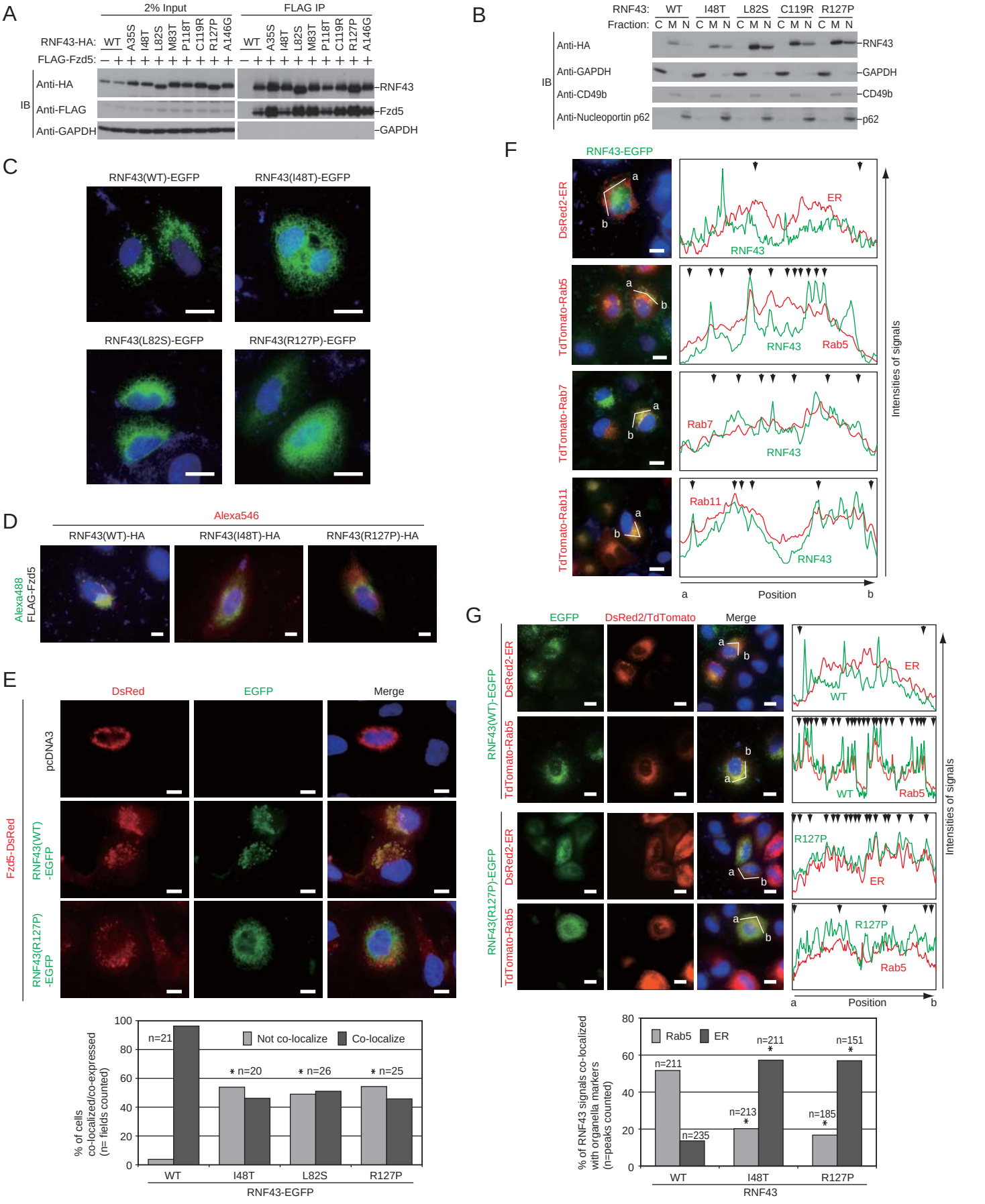

Tsukiyama_Figure 4

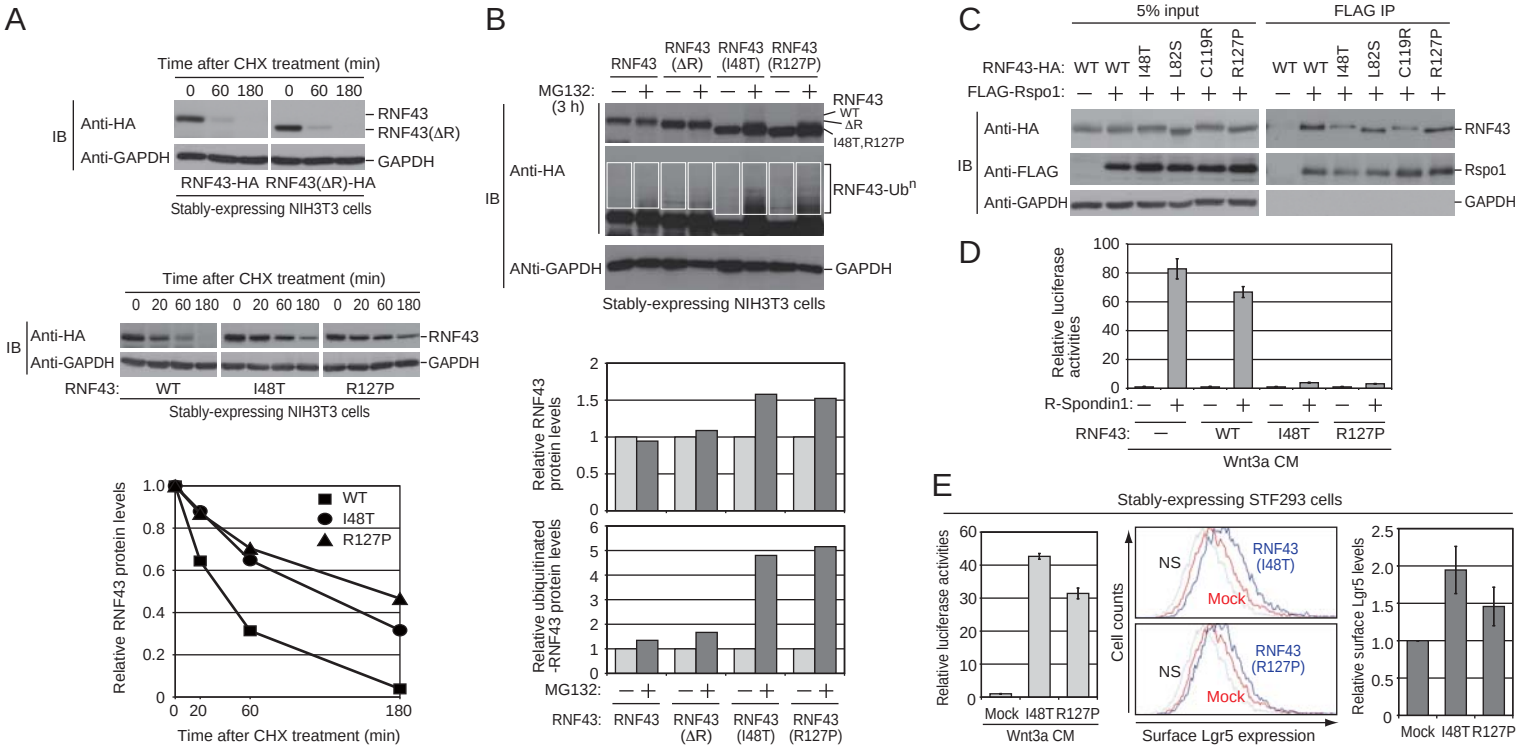

Tsukiyama_Figure 5

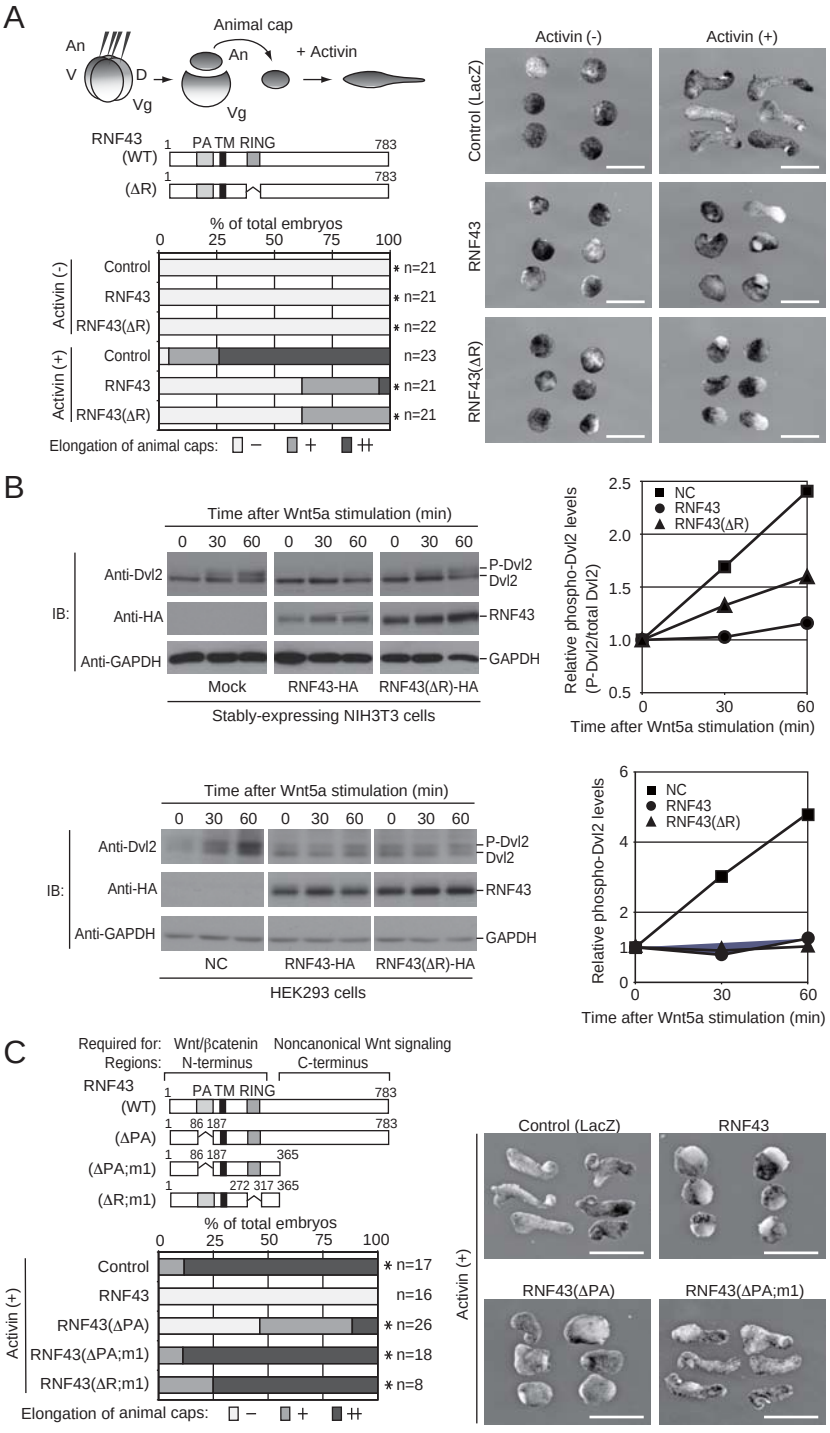
A
Animal cap
An
V
D
Vg
An
+ Activin
Vg
RNF43
(WT)
PA TM RING
1
783
(ΔR)
% of total embryos
0
25
50
75
100
Activin (-)
Control
RNF43
RNF43(ΔR)
Activin (+)
Control
RNF43
RNF43(ΔR)
n=21
n=21
n=22
n=23
n=21
n=21
Elongation of animal caps: − + ++
Activin (-)
Activin (+)
Control (LacZ)
RNF43
RNF43(ΔR)
B
Time after Wnt5a stimulation (min)
0 30 60 0 30 60 0 30 60
IB:
Anti-Dvl2
Anti-HA
Anti-GAPDH
P-Dvl2
Dvl2
RNF43
GAPDH
Mock
RNF43-HA
RNF43(ΔR)-HA
Stably-expressing NIH3T3 cells
NC
RNF43
RNF43(ΔR)
Relative phospho-Dvl2 levels
(P-Dvl2/total Dvl2)
Time after Wnt5a stimulation (min)
HEK293 cells
C
Required for:
Wnt/βcatenin
Noncanonical Wnt signaling
Regions:
N-terminus
C-terminus
RNF43
(WT)
(ΔPA)
(ΔPA;m1)
(ΔR;m1)
1
86
187
272
317
365
783
% of total embryos
Control
RNF43
RNF43(ΔPA)
RNF43(ΔPA;m1)
RNF43(ΔR;m1)
n=17
n=16
n=26
n=18
n=8
Elongation of animal caps: − + ++
Activin (+)
Control (LacZ)
RNF43
RNF43(ΔPA)
RNF43(ΔPA;m1)

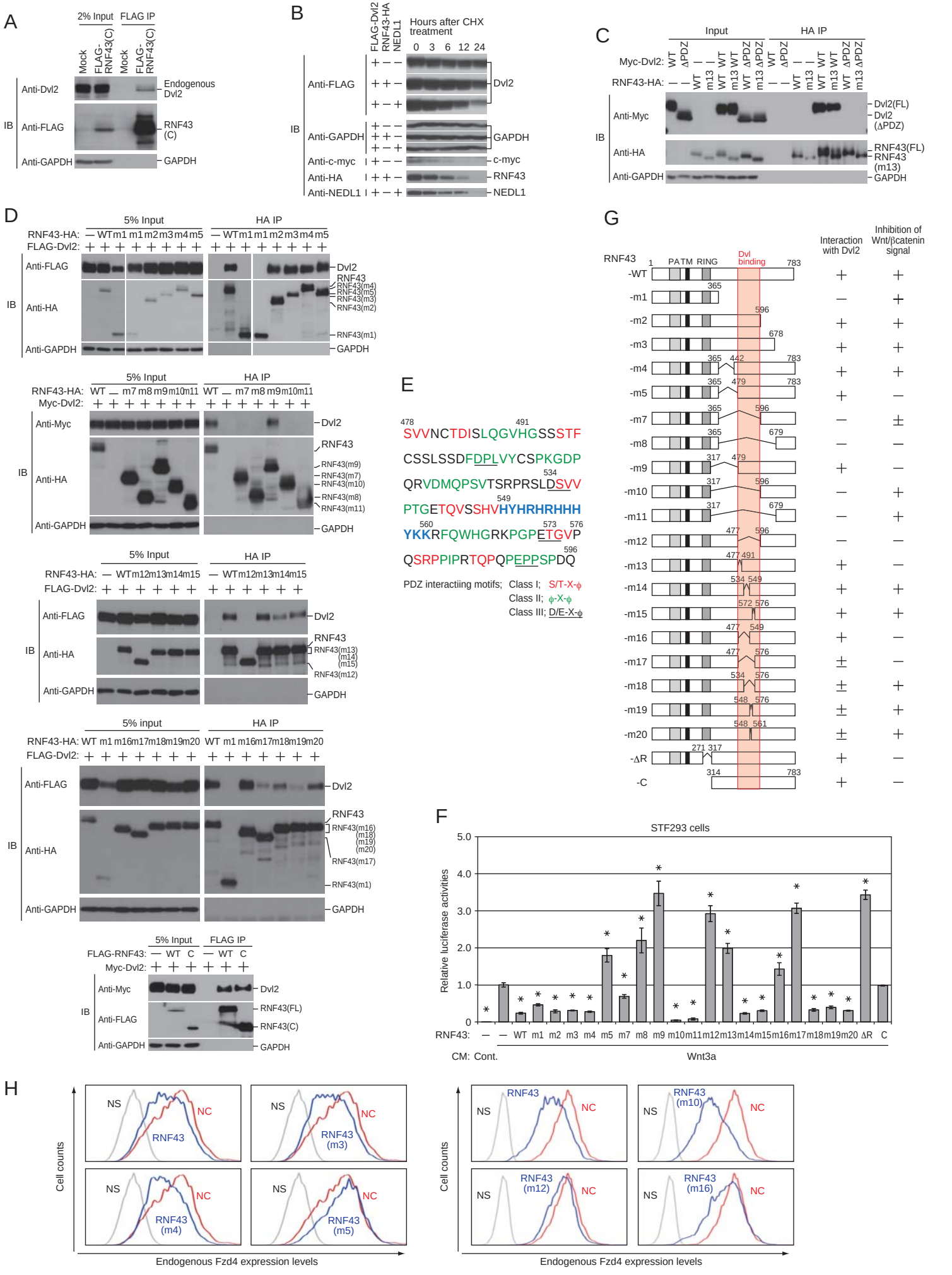

Tsukiyama_Figure 7

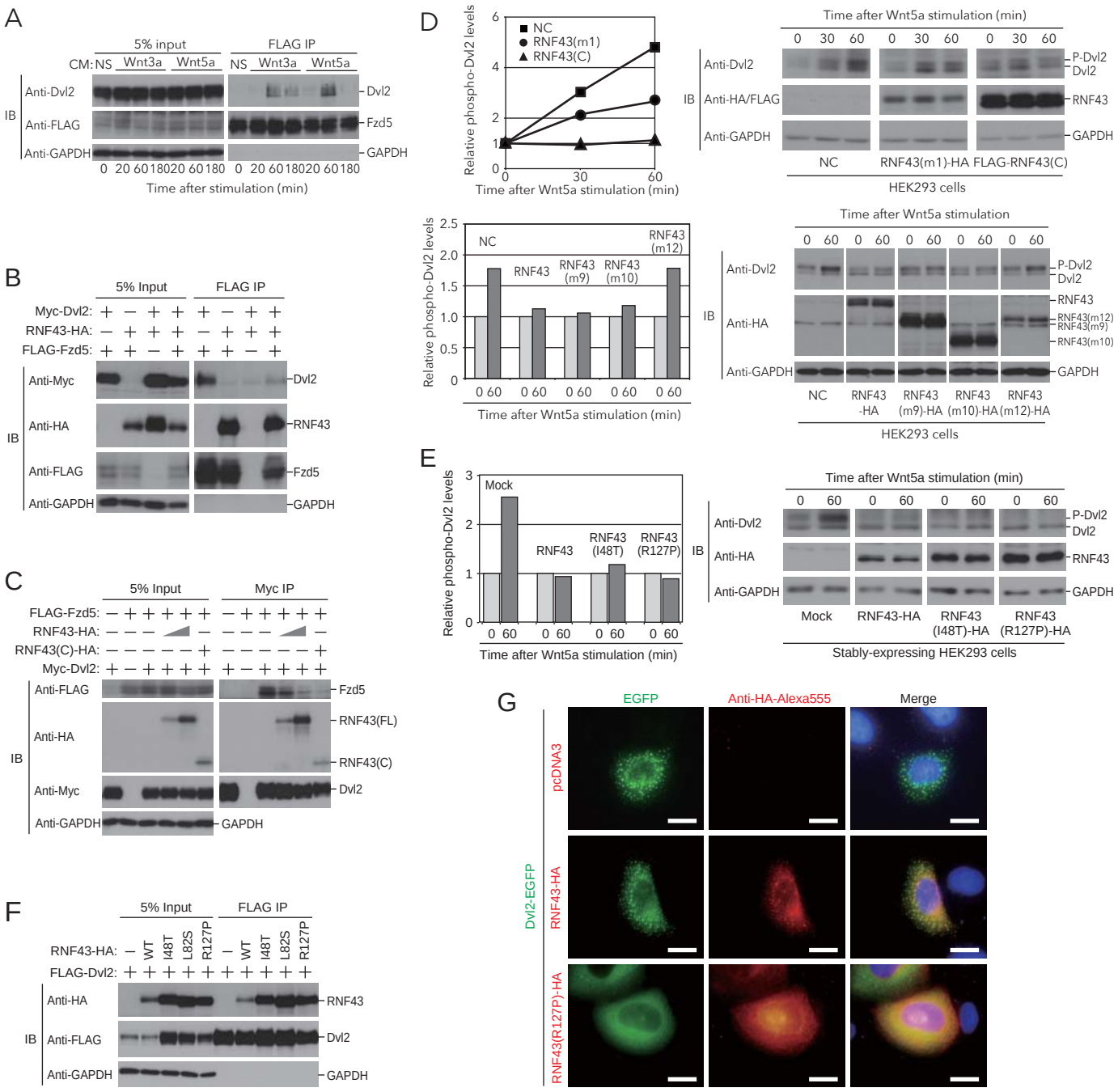
A
5% input
FLAG IP
CM: NS Wnt3a Wnt5a NS Wnt3a Wnt5a
IB
Anti-Dvl2
Anti-FLAG
Anti-GAPDH
Dvl2
Fzd5
GAPDH
0 20 60 180 20 60 180 0 20 60 180 20 60 180
Time after stimulation (min)
B
5% Input
FLAG IP
Myc-Dvl2:
RNF43-HA:
FLAG-Fzd5:
Anti-Myc
Anti-HA
Anti-FLAG
Anti-GAPDH
Dvl2
RNF43
Fzd5
GAPDH
C
5% Input
Myc IP
FLAG-Fzd5:
RNF43-HA:
RNF43(C)-HA:
Myc-Dvl2:
Anti-FLAG
Anti-HA
Anti-Myc
Anti-GAPDH
Fzd5
RNF43(FL)
RNF43(C)
Dvl2
GAPDH
D
NC
RNF43(m1)
RNF43(C)
Relative phospho-Dvl2 levels
Time after Wnt5a stimulation (min)
Time after Wnt5a stimulation (min)
0 30 60 0 30 60 0 30 60
Anti-Dvl2
Anti-HA/FLAG
Anti-GAPDH
P-Dvl2
Dvl2
RNF43
GAPDH
NC
RNF43(m1)-HA
FLAG-RNF43(C)
HEK293 cells
NC
RNF43
RNF43 (m9)
RNF43 (m10)
RNF43 (m12)
Time after Wnt5a stimulation (min)
Time after Wnt5a stimulation
0 60 0 60 0 60 0 60 0 60
Anti-Dvl2
Anti-HA
Anti-GAPDH
P-Dvl2
Dvl2
RNF43
RNF43(m12)
RNF43(m9)
RNF43(m10)
GAPDH
NC
RNF43 -HA
RNF43 (m9)-HA
RNF43 (m10)-HA
RNF43 (m12)-HA
HEK293 cells
E
Mock
RNF43
RNF43 (I48T)
RNF43 (R127P)
Relative phospho-Dvl2 levels
Time after Wnt5a stimulation (min)
Time after Wnt5a stimulation (min)
0 60 0 60 0 60 0 60
Anti-Dvl2
Anti-HA
Anti-GAPDH
P-Dvl2
Dvl2
RNF43
GAPDH
Mock
RNF43-HA
RNF43 (I48T)-HA
RNF43 (R127P)-HA
Stably-expressing HEK293 cells
F
5% Input
FLAG IP
RNF43-HA: – WT I48T L82S R127P – WT I48T L82S R127P
FLAG-Dvl2:
Anti-HA
Anti-FLAG
Anti-GAPDH
RNF43
Dvl2
GAPDH
G
EGFP
Anti-HA-Alexa555
Merge
Dvl2-EGFP
pcDNA3
RNF43-HA
RNF43(R127P)-HA

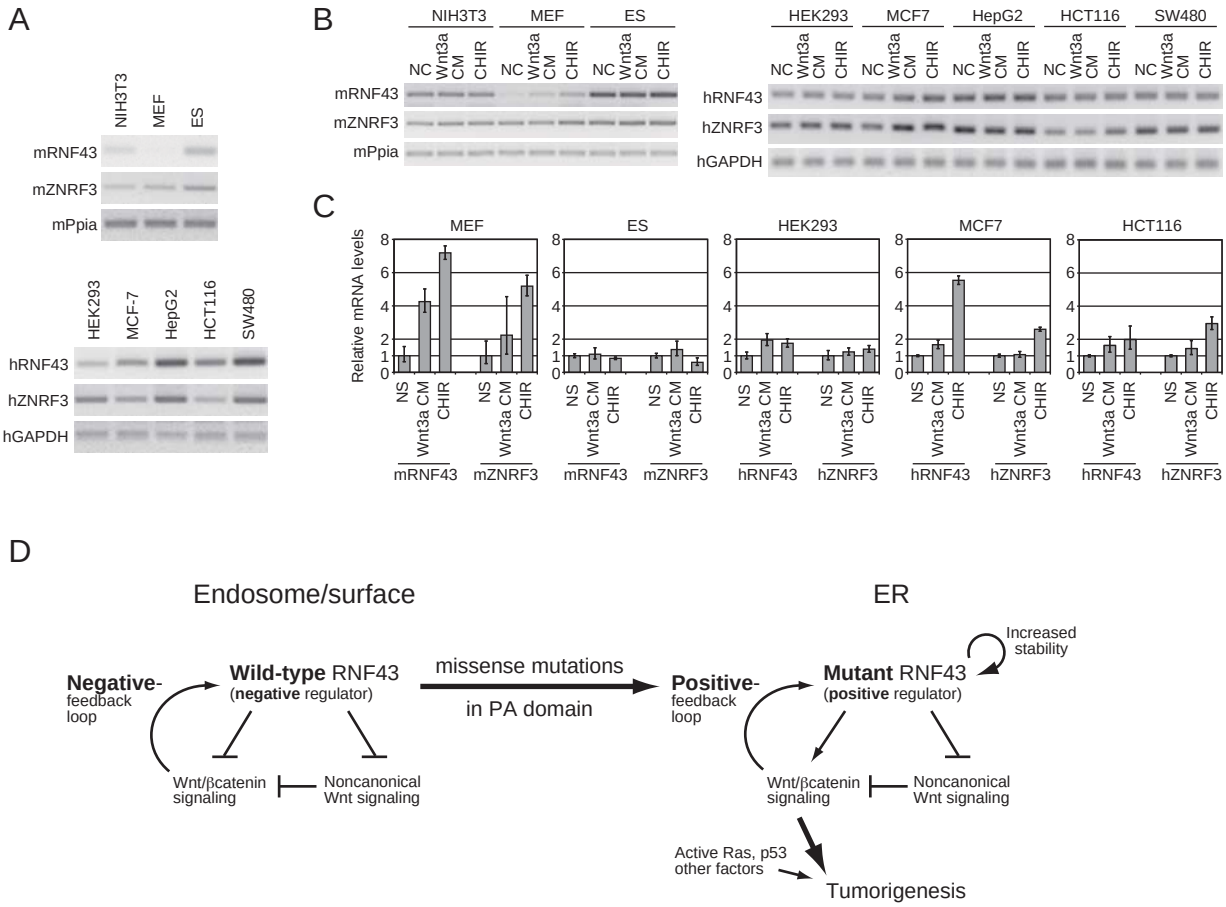

Tsukiyama_Figure 9

TABLE 1 Role of RNF43 in Wnt signaling in *Xenopus laevis* embryos

RNA	n=	Score of 2º axis	Complete 2º axis	Partial 2º axis	Single axis	Score of short axis	Short axis
GFP (1 ng)	63	0 ± 0.00	0	0	63	0 ± 0.00	0
xWnt8 (10 pg)	43	1.63 ± 0.11	32	6	5	N.C.	N.C.
xWnt8 (10 pg) + RNF43 (1 ng)	47	0.02 ± 0.02*	0	1	46	N.C.	N.C.
RNF43 (1 ng)	48	0 ± 0.00	0	0	48	0.66 ± 0.07**	32
RNF43(I48T) (1ng)	23	0 ± 0.00	0	0	23	0.13 ± 0.07**	3
RNF43(L82S) (1ng)	20	0 ± 0.00	0	0	20	0.20 ±0.09**	4
RNF43(R127P) (1 ng)	40	0 ± 0.00	0	0	40	0.08 ± 0.04**	3
xWnt8 (0.2 pg)	60	0.37 ± 0.08*	3	16	41	N.C.	N.C.
xWnt8 (0.2 pg) + RNF43(I48T) (1 ng)	41	1.34 ± 0.10***	18	19	4	N.C.	N.C.
xWnt8 (0.2 pg) + RNF43(L82S) (1 ng)	22	1.82 ± 0.08***	18	4	0	N.C.	N.C.
xWnt8 (0.2 pg) + RNF43(R127P) (1 ng)	43	1.63 ± 0.09***	29	12	2	N.C.	N.C.

Indicated combinations of mRNAs were injected into ventral blastomeres at the 4-cell stage as illustrated in Fig. 1G and 3E. The phenotypes of mRNA-injected embryos were evaluated at stage 37-38. Scores are calculated as described previously (21) with three

independent experiments and are presented as mean ± s.e. Asterisks indicate significant difference ($P < .05$, ANOVA) to xWnt8 (10 pg)-injected embryos (single), to GFP-injected control embryos (double) or to xWnt8 (0.2 pg)-injected embryos (triple). N.C., not counted.

Vector	Template	Forward primer	Sequence	Reverse primer	Sequence
pCR-FLAG-RNF43(C)	pcDNA3-RNF43	RNF43(C)-Fw	5’-ATGTTCAACATCACAGAGGGAG-3’	RNF43(C)-Rv	5’-TCACACAGCCTGTTCACACAGCTC-3’
pcDNA3-RNF43(ΔR)-HA		RNF43(ΔR)-Fw	5’-ATGTTCAACATCACAGAG-3’	RNF43(ΔR)-Rv	5’-CACAGGGGCTGAGCTGCAG-3’
pcDNA3-RNF43(m1)-HA		RNF43(m)-Fw	5’-CAGCCTGGCTCAGAGGAGGAAC-3’	RNF43(m1)-Rv	5’-ACCCTCGAGTGCACTCCGGGAAGGGCC-3’
pcDNA3-RNF43(m2)-HA		RNF43(m)-Fw	5’-CAGCCTGGCTCAGAGGAGGAAC-3’	RNF43(m2)-Rv	5’-ACCCTCGAGCTGATCAGGAGAAGGTGG-3’
pcDNA3-RNF43(m3)-HA		RNF43(m)-Fw	5’-CAGCCTGGCTCAGAGGAGGAAC-3’	RNF43(m3)-Rv	5’-ACCCTCGAGGCAAGCTGGGTGCACAGT-3’
pcDNA3-RNF43(m4)-HA		RNF43(m4)-Fw	5’-GACAGCAGTGGATCTGGAGAAAGC-3’	RNF43(m1)-Rv	5’-ACCCTCGAGTGCACTCCGGGAAGGGCC-3’
pcDNA3-RNF43(m5)-HA		RNF43(ΔDSG2)-Fw	5’-GTGGTCAACTGCACGGACATCAGC-3’	RNF43(m1)-Rv	5’-ACCCTCGAGTGCACTCCGGGAAGGGCC-3’
pcDNA3-RNF43(m7)-HA		RNF43(m7)-Fw	5’-CAAGTCACCAGATCCAACTCAG-3’	RNF43m1(365)new-Rv	5’-TGCACTCCGGGAAGGGCCCAAC-3’
pcDNA3-RNF43(m8)-HA		RNF43m8(678)-Fw	5’-CAGATTTTTCCCCATTACACCC-3’	RNF43m1(365)new-Rv	5’-TGCACTCCGGGAAGGGCCCAAC-3’
pcDNA3-RNF43(m9)-HA		RNF43(ΔDSG2)-Fw	5’-GTGGTCAACTGCACGGACATCAGC-3’	RNF43m(R-316)-Rv	5’-TGTGATGTTGAACATGCAGAG-3’
pcDNA3-RNF43(m10)-HA		RNF43(m7)-Fw	5’-CAAGTCACCAGATCCAACTCAG-3’	RNF43m(R-316)-Rv	5’-TGTGATGTTGAACATGCAGAG-3’
pcDNA3-RNF43(m11)-HA		RNF43m8(678)-Fw	5’-CAGATTTTTCCCCATTACACCC-3’	RNF43m(R-316)-Rv	5’-TGTGATGTTGAACATGCAGAG-3’
pcDNA3-RNF43(m12)-HA		RNF43(m7)-Fw	5’-CAAGTCACCAGATCCAACTCAG-3’	RNF43(m12)-Rv	5’-GTCACTGGAAGAGCCATGACA-3’
pcDNA3-RNF43(m13)-HA		RNF43(m13)-Fw	5’-AGCCTACAGGGGGTCCATGGC-3’	RNF43(m12)-Rv	5’-GTCACTGGAAGAGCCATGACA-3’
pcDNA3-RNF43(m14)-HA		RNF43(m14)-Fw	5’-CACTACCACCGCCACCGGCAC-3’	RNF43(m14)-Rv	5’-GTCCAAGGAACGAGGCCGAGAG-3’
pcDNA3-RNF43(m15)-HA		RNF43(m15)-Fw	5’-CCCCAGTCCAGGCCTCCTATTC-3’	RNF43(m15)-Rv	5’-TTCTGGGCCAGGCTTCCTG-3’
pcDNA3-RNF43(m16)-HA		RNF43(m14)-Fw	5’-CACTACCACCGCCACCGGCAC-3’	RNF43(m12)-Rv	5’-GTCACTGGAAGAGCCATGACA-3’
pcDNA3-RNF43(m17)-HA	pcDNA3-RNF43-HA	RNF43(m15)-Fw	5’-CCCCAGTCCAGGCCTCCTATTC-3’	RNF43(m12)-Rv	5’-GTCACTGGAAGAGCCATGACA-3’
pcDNA3-RNF43(m18)-HA		RNF43(m15)-Fw	5’-CCCCAGTCCAGGCCTCCTATTC-3’	RNF43(m14)-Rv	5’-GTCCAAGGAACGAGGCCGAGAG-3’
pcDNA3-RNF43(m19)-HA		RNF43(m19)-Fw	5’-ACCGGAGTCCCCCAGTCCAG-3’	RNF43(m19)-Rv	5’-GACATGGCTGGAAACCTG-3’
pcDNA3-RNF43(m20)-HA		RNF43(m20)-Fw	5’-CGGTTCCAGTGGCATGGCAG-3’	RNF43(m19)-Rv	5’-GACATGGCTGGAAACCTG-3’
pcDNA3-RNF43(ΔCPD)-HA		RNF43(m)-Fw	5’-CAGCCTGGCTCAGAGGAGGAAC-3’	RNF43(ΔCPD)-Rv	5’- CTGGCTGATGGCCCAGGCTGTTCT-3’
pcDNA3-RNF43(ΔPA)-HA		RNF43(ΔPA)-Fw	5’- GAGCTGAAGGAGCCCCCGGCCTGG-3’	RNF43(ΔPA)-Rv	5’- GTGGGACTGCATTAATTTTCCTTC-3’
pcDNA3-RNF43(A35S)-HA		RNF43(A35S)-Fw	5’-TCGGTGGAGTCTGAAAGATCAG-3’	RNF43(A35S)-Rv	5’-TGCTGCCAGTACCAGTCCTGTG-3’
pcDNA3-RNF43(I48T)-HA		RNF43(I48T)-Fw	5’-CCAGAGTGATCCCCTTGAAAATG-3’	RNF43(I48T)-Rv	5’-TAATAGCTTTCTGTTCTGCTG-3’
pcDNA3-RNF43(L82S)-HA		RNF43(L82S)-Fw	5’-CAATGCAGTCCCACCCGCTGTAC-3’	RNF43(L82S)-Rv	5’-ATTTTCCTTCTGCTGGAGTTATTTC-3’
pcDNA3-RNF43(M83T)-HA		RNF43(M83T)-Fw	5’-CGCAGTCCCACCCGCTGTACCTG-3’	RNF43(M83T)-Rv	5’-TTAATTTTCCTTCTGCTGGAG-3’
pcDNA3-RNF43(P118T)-HA		RNF43(P118T)-Fw	5’-ACCTGCCTGTCACTGGCTAGC-3’	RNF43(P118T)-Rv	5’-GCGGGGGGCCCGTCGAGGACTC-3’
pcDNA3-RNF43(C119R)-HA		RNF43(C119R)-Fw	5’-CGCCTGTCACTGGCTAGCAAGGC-3’	RNF43(C119R)-Rv	5’-GGGGCGGGGGGCCCGTCGAGGAC-3’
pcDNA3-RNF43(R127P)-HA		RNF43(R127P)-Fw	5’-CGATGGCGGGTGAGCGAGGAGCC-3’	RNF43(R127P)-Rv	5’-GAGCCTTGCTAGCCAGTGACAG-3’
pcDNA3-RNF43(A146G)-HA		RNF43(A146G)-Fw	5’-GTGCTGCTGAGCAGCTGCAGCAGC-3’	RNF43(A146G)-Rv	5’-CTCGATCCTCAGTGATGTCAAAG-3’
pcDNA3-RNF43(N167I)-HA		RNF43(N167I)-Fw	5’-TTGACGCTGAGAAGCTGATGGAG-3’	RNF43(N167I)-Rv	5’-TACCCCAGATCAACACCACTGGC-3’
pcDNA3-RNF43(A169T)-HA		RNF43(A169T)-Fw	5’-ACTGAGAAGCTGATGGAGTTTGTG-3’	RNF43(A169T)-Rv	5’-GTCATTACCCCAGATCAACACCAC-3’
pcDNA3-RNF43(T204R)-HA		RNF43(T204R)-Fw	5’-GAGTGGTGGGCACCATCTTTGTG-3’	RNF43(T204R)-Rv	5’-TCATTAGGATCCACACATCATAATC-3’
pcDNA3-RNF43(S216L)-HA		RNF43(S216L)-Fw	5’-TGGTGCTGCGCATCCGGTGCCGCC-3’	RNF43(S206L)-Rv	5’-AAGCCAGGATGATCACAAAGATG-3’
pMX-puro-RNF43(si mt)-HA	pMX-puro-RNF43-HA				
pMX-puro-RNF43(I48T;si mt)-HA	pMX-puro-RNF43(I48T)-HA	RNF43-(si mt)-Fw	5'-TATTGTACAGAACGCAGTGGG-3'	RNF43-(si mt)-Fw	5'-GCTCTCTCCAGATCCACTGCTG-3'
pMX-puro-RNF43(R127P;si mt)-HA	pMX-puro-RNF43(R127P)-HA				
pCS2-FLAG-Fzd5	pCS2-Fzd5	FLAG-Fzd5-Fw	5’-TCCGACTACAAGGACGACGATGACAAGGACGACTACAAGGACGACGATGACAAGTCCAAGGCCCCGGTGTGCCAGGAA-3’	FLAG-Fzd5-Rv	5’- GGCGGCCGCTGCCCGGCCCACCAGC-3’
pCS2-FLAG-Fzd5(ΔCRD)	pCS2-FLAG-Fzd5	Fzd5(ΔCRD)-Fw	5’-ACCGCGTCCCCTAAGTCCTTCCCG-3’	Fzd5(ΔCRD)-Rv	5’-TTCCTGGCACACCGGGGCCTTGGA-3’
pCS2-FLAG-Fzd5(CRD)	pCS2-FLAG-Fzd5	Fzd5(CRD)-Fw	5’-AACAAGCTTACCATGGCTCGACCCGACCCGTCTGCG-3’	Fzd5(CRD)-Rv	5’-AACGAATTCCTAGGTGGCTTCGCTTCGGTTATAATC-3’
pFLAG-CMV-hRspo1	human prostate cDNA	hRspo1-Fw	5’-ACCGAATTCACCATGCGGCTTGGGCTGTGTGTG-3’	hRspo1-Rv	5’-ACCGGATCCGGCAGGCCCTGCAGATGTGAGTG-3’

Table S1. List of primers and templates to generate the indicated vectors.